DOSE PROFILE AND UNCERTAINTY ANALYSIS OF NARROW BEAM X-RAYS AND COLLIMATED ^{137}Cs SOURCE USED AT THE SECONDARY STANDARDS DOSIMETRY LABORATORY OF THE GHANA ATOMIC ENERGY COMMISSION

A THESIS PRESENTED TO THE

DEPARTMENT OF MEDICAL PHYSICS

GRADUATE SCHOOL OF NUCLEAR AND ALLIED SCIENCES

UNIVERSITY OF GHANA

BY

JOHN JABATI

(10361522)

IN PARTIAL FULFILMENT OF THE REQUIREMENTS FOR THE AWARD OF MASTER OF PHILOSOPHY DEGREE

IN

NUCLEAR SCIENCE AND TECHNOLOGY

JUNE, 2013

DECLARATION

Candidate's Declaration:

I hereby declare that, with exception of references to other people's work which have duly been acknowledged, this work is the result of my own original research undertaken under supervision, and either in whole or in part has not been presented for any other degree at another university elsewhere.

…… …….

John Jabati Date

(Student)

Supervisors' Declaration:

We hereby declare that the preparation and presentation of the thesis were supervised in accordance with guidelines on supervision of thesis laid down by the University of Ghana, Legon.

…… ……

Prof. Emmanuel Ofori Darko Date

(Principal Supervisor)

…… ……

Dr. Joseph Kwabena Amoako Date

(Co-supervisor)

DEDICATION

This work is first of all dedicated to the Almighty God for giving me the grace to successfully complete it.

Furthermore, I dedicate this work with my deepest gratitude to my parents, Mr. Francis K. Jabati and Mrs. Rosaline Satta Jabati for their encouragement and support and to my dear wife Mrs. Nanette Salome Jabati for her constant love and cooperation.

ACKNOWLEDGEMENT

My profound gratitude and thanks go to the Almighty God whose love, mercy, guidance and protection has brought me this far.

I wish to acknowledge with sincere gratitude my supervisors and mentors, Prof. Emmanuel Ofori Darko, Deputy Director of Radiation Protection Institute and Dr. Joseph Kwabena Amoako, Manager, Health Physics and Instrumentation Centre who through their patience and meticulous supervision and advice have seen this project come into a reality.

My sincere appreciation also go to the Management of Ghana Atomic Energy Commission and the Radiation Protection Institute for making available their facilities to be used for the study and to Mr. James Annkah, Mr. Daniel Adjei and Mr. Michael K. A. Obeng for their individual contributions and technical assistance.

My special thanks also go to Prof. Cyril Schandorf, Department of Nuclear Safety and Security and Prof. J. J. Fletcher for many technical recommendations and contribution of materials and to the staff of Personnel Monitoring Service Laboratory especially Mr. Philip Owusu-Manteaw for his contributions and corporation.

I am deeply indebted to Mr. Josephus J. Kongo, Chief Radiation Protection Officer and Executive Director of Nuclear Safety and Radiation Protection Authority, for nominating me for this course on behalf of the government of Sierra Leone and finally to the International Atomic Energy Agency for awarding me the fellowship to pursue this programme.

TABLE OF CONTENTS

LIST OF TABLES

Table **Page**

Table **Page**

LIST OF FIGURES

Figure **Page**

Figure **Page**

LIST OF PLATES

Plate **Page**

LIST OF ABBREVIATIONS

ALARA	As Low As Reasonably Achievable
BIPM	Bureau International des Poids et Measures
CCTV	Closed Circuit Television
GAEC	Ghana Atomic Energy Commission
GM	Geiger Muller
HVL	Half Value Layer
IAEA	International Atomic Energy Agency
ICRU	International Commission on Radiation Units and Measurements
IEC	International Electrotechnical Commission
ISO	International Organisation for Standardization
IUPAP	International Union of Pure and Applied Physics
OIML	International Organization of Legal Metrology
PSDL	Primary Standard Dosimetry Laboratory
RPP	Radiation Protection Programme
RPO	Radiation Protection Officer
SSDL	Secondary Standard Dosimetry Laboratory
TLD	Thermoluminescent Dosimeter
WHO	World Health Organisation

LIST OF SYMBOLS AND CONSTANTS

Symbol	Meaning	Unit
λ	Decay constant	s^{-1}
N_k	Calibration coefficient	$(\mu Gy/nC)$
μ	Linear attenuation coefficient	cm^{-1}
ρ	Physical density	kgm^{-3}
γ	Gamma radiation	
E	Photon energy	MeV
c	Speed of light	$(3\times10^{8})\ ms^{-1}$
μ/ρ	Mass attenuation coefficient	$cm^{2}g^{-1}$
$\mathring{A}$	Angstrom	$10^{-10}\ m$
ϕ	Particle fluence	m^{-2}
$\dot{\phi}$	Particle fluence rate	$m^{-2}s^{-1}$
ψ	Energy fluence	Jm^{-2}
$\dot{\psi}$	Energy fluence rate	Wm^{-2} or $Jm^{-2}s^{-1}$

ABSTRACT

The study highlighted the importance of dose standardization to ensure that radiation measurements are linked to the international system. The half value layer (HVL) was determined and compared with ISO 4037 values and the values quoted on the calibration certificate of the reference ionization chamber to verify whether the X-ray machine is emitting correct energies. The percentage (%) deviation of the HVL obtained for the various X-ray emitting beam qualities are within the acceptable limits except for the 60 kV which was subsequently modified by using 0.7 mm Al. The dose profiles for the narrow beam X-rays and the collimated ^{137}Cs source were established. The difference resulting from the theoretical and measured values is generally less than 10% in the useful range of 1 to 2m. The dose profiles generated provides standardized beam output characteristics that can be used to calibrate dose rate monitoring equipment, TLDs and other dosimetry systems. The uncertainty analysis indicated that most of the calibration factors with the associated uncertainties for the set of survey meters calibrated at the Secondary Standards Dosimetry Laboratory of Ghana Atomic Energy Commission are within the acceptable limits. The uncertainties ranged from 0.03 to 17% with the majority of them ranging from 0.03 to 6.0 % with only a few of them more than 6.0 %.

CHAPTER ONE

INTRODUCTION

1.1 Background

The applications of radiation and radioisotopes range from life-saving medical procedures to material characterization and food preservation (Lamash et al, 2001). However, the risks associated with radiation and radioactive materials must be restricted and protected against by the application of appropriate radiation safety standards (IAEA, 1996). Radiation is classified into ionizing and non-ionizing, depending on its ability to ionize matter. The ionization potential of atoms ranges from a few electronvolts (eV) for alkali elements to 24.5 eV for helium. Ionizing radiation can ionize matter either directly or indirectly (IAEA, 2005).

Radiation monitoring of the working environment and the surrounding areas is an essential part of any effective radiation protection programme to ensure that neither the operating personnel nor the general population receives radiation doses in excess of dose limits (IAEA, 1996; Adjei et al, 2012).

Radiation protection instruments are important operational tools that fulfil radiation safety requirements and therefore very important to test their performance to meet the required accuracy and intended use. Periodic calibration ensures traceability of chain of measurements to the international measurement system (IAEA, 2000; Kramers, 1992; De Freitas et al, 1992; Annkah et al, 2011).

Calibration is the quantitative determination, under a controlled set of standard conditions, of the indication given by a radiation measuring instrument as a function of the value of the quantity the instrument is intended to measure (IAEA, 2000). In general, it is a procedure for establishing a relationship between the indicated value of

a measuring instrument and the conventional true value of the quantity to be measured under well-defined reference conditions (Stadtmann, 2001). Calibration is therefore necessary in order to ensure that appropriate levels of accuracy and long term reproducibility of dose measurements are maintained (Sulimanet al, 2010; Stadtmann, 2001).

The International Atomic Energy Agency (IAEA) and the World Health Organization (WHO) created a network of Secondary Standard Dosimetry Laboratories (SSDLs) in 1976 (IAEA, 2009) to improve dosimetric accuracy in radiation dosimetry. The SSDL Network has the responsibility to assure that the services provided by the laboratory members follow internationally accepted metrological standards. At present, this is achieved by providing traceable calibrations for therapy, radiation protection and diagnostic radiology instruments by the IAEA. The dosimetry laboratory of the IAEA is the central laboratory of the IAEA/WHO network of SSDLs. It provides calibration services to the SSDL members. The dosimetry laboratory is operated following a peer-reviewed quality system based on the International Organization for Standardization ISO 17025. An SSDL is equipped with secondary standards which are traceable to the primary standard dosimetry laboratories (PSDLs) or the Bureau International des Poids et Mesures (BIPM) (IAEA, 2008).The traceability is accomplished first with the dissemination of calibration factors for ionization chambers from the BIPM or PSDLs through the IAEA. As a second step, follow-up programmes and dose quality audits (intercomparisons using ionization chambers and TLDs) are implemented for the SSDLs to assure that the standards transmitted to users in Member States are kept within the levels required by the International Measurement System (IAEA, 1999).

In achieving its mandate of the International Basic Safety Standard, the IAEA has supported projects for the establishment of ionizing radiation calibration laboratories in developing countries. Such facilities play a key role in the protection of staff, public and environment from the harmful effects of ionizing radiation (Sulimanet al, 2010), and so satisfy the regulatory requirements imposed by the relevant authority in the country. This has an implication that pre defined dose limits for both occupational and public exposures recommended by the International Commission on Radiological Protection are not exceeded (ICRP,1991; 2007).

In Ghana, calibration of radiation measuring instruments is a legal requirement under the Radiation Protection Instrument, (LI 1559 of 1993). The Secondary Standards Dosimetry Laboratory (SSDL) which was established in 1988 by GAEC under the IAEA Technical Co-operation project number GHA/1/007is part of the network of the WHO and IAEA SSDLs distributed worldwide. The SSDL has been designated as the National Radiation Calibration Laboratory, which undertakes calibration services and act as a link in the traceability chain to the international measurement system for radiation metrology users. The SSDL is located at the Radiation Protection Institute of the Ghana Atomic Energy Commission (GAEC) and is traceable to the Austrian National Primary Standards Laboratory in Vienna. The role of the Ghana SSDL is crucial in providing traceable calibrations, disseminating calibrations at specific radiation qualities appropriate for the use of radiation measuring instruments and issue statements regarding the uncertainty of this calibration. The SSDL also provides technical information and conduct long-term studies of dosimetry system characteristics, such as environmental effects and evaluate new, emerging dosimetry systems to assist in technology transfer to industry, medicine, agriculture and research laboratories (Adjeiet al, 2013).

Although International intercomparisons of these standards have exhibited very good agreement, a substantial weakness prevails in that all such standards are based on ionization chambers and are therefore subject to common errors. In addition, depending on the method of evaluation, a factor related to the attenuation in the chamber wall entering into the determination of the quantity air kerma has been found to differ by up to 0.7% for some primary standards(IAEA, 2000).

The IAEA intercomparison programme with transfer ionization chambers includes the measurement of calibration coefficients for air kerma and absorbed dose to water in ^{60}Co or ^{137}Cs gamma radiation. The results of the comparisons are confidential and are communicated only to the participants. This confidentiality is to encourage the participation of the laboratories and their full cooperation in the reconciliation of any discrepancy (IAEA, 2009).

1.2 Statement of the Problem

The safe use of ionising radiation requires accurate measurements that are traceable to national and international standards (McDonald, 2004). It is a regulatory requirement that all survey meters for radiation protection purposes be tested and calibrated to ensure that their performance meet the required accuracy and intended use (Adjei et al, 2013).

Since the commissioning of the SSDL in 1988 a consistent follow-up of whether the X-ray radiation qualities and dose profiles used for calibration has maintained a consistent performance with recent power cuts and fluctuations and environmental conditions of the Laboratory. Hence the need to revalidate these parameters.

The ^{137}Cs panoramic Irradiator configuration has been modified to provide a collimated beam for calibration. This exposure configuration demands new studies on the beam profiling and establishing of air kerma rate measurements for accurate and reliable dosimetry work.

1.3 Objectives of the Study

The main objective of this study is to establish dose profiles for the narrow beam x-rays and collimated^{137}Cssource at the SSDL in GAEC.

The specific objectives include the following:

1. To measure the half value layer (HVL) for all x-ray beam qualities available.
2. To modify the X-ray beam to agree with ISO 4037 values using added filtration.
3. To determine the extent of the X- ray beam consistency.
4. To generate reference values (Air kerma rates and Ambient dose equivalent) that will serve as standards for calibration of radiation monitoring equipment, irradiation of samples, TLDs and all dosimetric requirements at the SSDL in GAEC.
5. To analyse the uncertainty associated with the reference ambient dose measurements and the calibration of radiation survey meters.

1.4 Relevance and Justifications

The SSDL must have an X-ray beam quality that corresponds to ISO4037 values within acceptable limits of variation. This will ensure that all equipment calibrated at the SSDL will have traceability and accuracy. It will also ensure harmonization and consistency in radiation measurements. To perform calibration we use the useable range of the equipment. If useable range is very low ($0-200\,\mu Svh^{-1}$) the ^{137}Cs source with energy $662\,keV,$ cannot be used for calibration. There is currently no available well established profile for the x-ray unit at the SSDL at GAEC. The SSDL facility at GAEC has been in existence for over twenty years and the ^{137}Cs source which was originally panoramic is now collimated. The establishment of the dose profile with the assessment of the quality control factors helps in calibrating survey meters at different energy levels. This must periodically be established. However, these assessments have not been fully implemented for some years now.

It is therefore important to carry out a comprehensive HVL and dose profile assessment in order to standardize and validate the facility. This research will enhance and improve calibration services performed by the SSDL and minimise errors accompanied by radiation exposure during calibration.

1.5 Scope and Limitations

The secondary standard dosimetry facility at GAEC was used for this experimental study. This includes the X-ray unit with a $320\,kV$ tube, the collimated ^{137}Cs gamma ray unit as well as the SSDL reference instrument. The SSDL reference instrument had been calibrated at the IAEA dosimetry laboratory (radiation protection

level calibration) for ^{137}Cs, ^{60}Co gamma and ISO4037 X-ray qualities (narrow-spectrum series).

1.6. Thesis Structure

This thesis has the following sections:

Chapter one is introduction of the thesis which provides adequate background information about the topic that enables the reader to understand the study. It states the nature of the problem to be investigated which will be developed further in subsequent chapters. It defines the objectives, justification and scope of the research undertaken.

Chapter two reviews existing literature relevant to the research problem.

Chapter three is the methodology which describes the procedures and equipment used in sufficient details to enable other researchers reproduce the results.

Chapter four is results and discussions and presents data from the study and emphasize on important observations made. This chapter also discusses the results obtained, brings out the new and important aspects of the study. It discusses the implications of the findings in relation to other relevant published studies. Show whether the results and interpretations agree or contrast with previously published work. The chapter also discusses the limitations of the experimental design and the achievement of the study objectives.

Chapter five gives conclusions and recommendations based on the study results.

CHAPTER TWO

LITERATURE REVIEW

This chapter provides a summary of the pertinent literature with respect to what is known about this topic of study. This includes photon interactions and dosimetric principles. This section also contains a brief review of the basis of radiation protection and the background theory on uncertainty of measurements and International guidance are presented.

2.1 Photon Interactions

Ionizing radiation transfers its energy in full or part to the medium through which it passes by way of interactions. The significant types of interactions are excitation and ionization of atoms or molecules of the matter by charged particles and electromagnetic radiation (x-rays or gamma rays) (Khalil, 2011).

2.1.1 Types of Photon Radiation

Depending on their origin, photon radiations fall into one of the following four categories:

i. Bremsstrahlung (continuous X-rays), emitted through electron–nucleus interactions.

ii. Characteristic X-rays (discrete), emitted in transitions of orbital electrons from one allowed orbit to a vacancy in another allowed orbit.

iii. Gamma rays (discrete), emitted through nuclear transitions in γ decay.

iv. Annihilation radiation (discrete, typically 0.511 MeV), emitted through positron-electron annihilation (IAEA, 2005).

2.1.2 Photon Beam Attenuation

The intensity $I_{(x)}$ of a narrow monoenergetic photon beam, attenuated by an attenuator of thickness x, is given by equation (2.1).

$$I_{(x)} = I_{(0)} e^{-\mu(h\upsilon, Z)x} \qquad (2.1)$$

Where $I_{(0)}$ is the original intensity of the unattenuated beam;

$\mu(h\upsilon, Z)$ is the linear attenuation coefficient, which depends on photon energy $h\upsilon$ and attenuator atomic number Z (IAEA, 2005, Smith, 2000; Knoll,1999; Lamash et al, 2001).

The half-value layer (HVL) of an X-ray beam is defined as the thickness of a specified attenuator that reduces the air-kerma rate in a narrow beam to one half its original value.

Hence,

$$HVL = \frac{\ln 2}{\mu} \qquad (2.2)$$

The determination of HVL involves the measurement of the variation with the attenuator thickness of air kerma at a point in a scatter free and narrow beam. This means that for this measurement, detectors shall be used with sufficient buildup thickness to eliminate the effect of contaminant electrons (Ma et al, 2001).

For the air-kerma measurement, small-size detectors are desirable. The beam must cover the sensitive volume of the detector. The detector response shall have limited beam-quality dependence ~within 5% between 40 and300 kV, for accurate *HVL* measurements. The attenuator shall be made of high-purity (~99.9%) material and the thickness of the attenuator shall be measured with an accuracy of0.05 mm (Ma et al, 2001).

2.1.3 Types of Photon Interaction

Photons may undergo various possible interactions with the atoms of an attenuator; the probability or cross-section for each interaction depends on the energy hυ of the photon and on the atomic number Z of the attenuator.

The photon interactions may be with a tightly bound electron i.e. with an atom as a whole (photoelectric effect, coherent scattering), with the field of the nucleus (pair production) or with an essentially free orbital electron (Compton effect, triplet production).

In the context of photon interactions, a tightly bound electron is an orbital electron with a binding energy of the order of, or slightly larger than, the photon energy, while a free electron is an electron with a binding energy that is much smaller than the photon energy. During the interaction the photon may completely disappear (photo-electric effect, pair production) or it may be scattered (Compton effect) (IAEA, 2005).

Gamma photons up to 3 MeV undergo compton interactions, photoelectric interactions and pair productions. With energies less than 1.022 MeV, Compton and

Pair production are possible. In the case of ^{137}Cs with a much lower energy of 0.662 MeV, Compton interaction is dominant (Smith, 2000).

Photons also undergo Rayleigh scattering, Bragg scattering, photodisintegration, and nuclear resonance scattering; however, these result in negligible attenuation or energy deposition and can generally be ignored for purposes of radiation protection (Martin, 2006).

2.1.3.1. The Photoelectric Effect

In the photoelectric effect (sometimes referred to as the photo-effect) the photon interacts with a tightly bound orbital electron of an attenuator and disappears, while the orbital electron is ejected from the atom as a photoelectron with a kinetic energy E_K given by equation (2.3).

$$E_K = h\upsilon - E_B \qquad (2.3)$$

Where $h\upsilon$ is the incident photon energy and E_B is the binding energy of the electron (IAEA, 2005; Knoll, 2000).The atom recoils in this process, but carries with it very little kinetic energy. The kinetic energy of the ejected photoelectron is therefore equal to the energy of the photon less the binding energy of the electron to the atom-that is, the ionization energy for the electron in question (Lamash et al, 2001).

X-rays and γ-rays not only exhibit "wave" properties like all frequencies of electromagnetic radiation but also exhibit discrete "particle" characteristics as described by quantum mechanics (thus, the word "photon"). Photoelectric absorption involves the interaction of an incident X-ray photon with an inner shell electron in the absorbing atom that has a binding energy similar to but less than the energy of the

incident photon. The incident X-ray photon transfers its energy to the electron and results in the ejection of the electron from its shell (usually the K shell) with a kinetic energy equal to the difference of the incident photon energy, $h\upsilon$ and the electron shell binding energy, E_B, as shown in Figure 2.1.

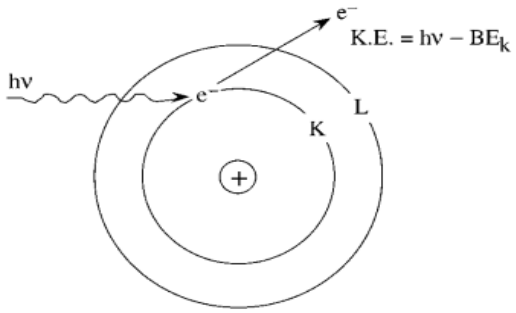

Figure 2.1: Schematic of the photoelectric effect.

The vacated electron shell is subsequently filled by an electron from an outer shell with less binding energy (e.g., from the L or M shell), producing a characteristic X-ray equal in energy to the difference in electron binding energies of the source electron shell and the final electron shell. If the incident photon energy is less than the binding energy of the electron, the photoelectric interaction cannot occur, but if the x-ray energy is equal to the electronic binding energy $(h\upsilon = E_B)$, the photoelectric effect becomes energetically feasible and a large increase in attenuation occurs. After photoelectric interaction, ionization of the atom occurs and a free photoelectron and a positively charged atom are produced. Kinetic energy of the ejected photoelectron can cause further electron–electron ionization, with most energy locally deposited. Also, a subsequent cascade of electron transitions to fill the vacated inner electron shell results in emission of characteristic radiation (Seibert et al, 2005; Knoll, 2000).

The probability of photoelectric absorption, commonly denoted as the symbol τ, is proportional to the cube of the atomic number of the interacting atom and inversely proportional to the cube of the energy, as Z^3/E^3. Photoelectric interaction is more likely to occur with higher atomic number elements and lower X-ray energies. (Seibert et al, 2005; Lamash et al, 2001).

The photoelectric absorption coefficient τ given by equation (2.4) is a function of the atomic number Z of the absorbing material (generally related to the density ρ of the absorbing medium) and the energy of the radiation.

$$\tau \cong k \times \frac{Z^5}{E^3} \qquad (2.4)$$

Where k is a constant.

It is evident that photoelectric absorption is most pronounced in high-Z materials and for low-energy photons (less than 0.5 MeV). In a high-Z material such as lead, L X-rays and M X-rays can also be prominent emissions from target atoms and these will either be absorbed in the absorbing medium or will contribute to the photon fluence (Martin, 2006).

2.1.3.2 The Compton Effect

The Compton effect, or Compton scattering as it is sometimes called is an inelastic interaction between an X-ray or γ-ray photon of energy E_0 that is much greater than the binding energy of an atomic electron (in this situation, the electron is essentially regarded as "free" and unbound). Partial energy transfer to the electron

causes a recoil and removal from the atom at an angle, φ. The remainder of the energy, E_S, is transferred to a scattered X-ray photon with a trajectory of angle θ relative to the trajectory of the incident photon. While the scattered photon may travel in any direction (i.e., scattering through any angle θ from 0^0 to 180^0), the recoil electron may only be directed forward relative to the angle of the incident photon (> 0^0 to $\sim 90^0$) (Seibert et al, 2005; Knoll, 2000; Lamash et al, 2001).

The Compton-scattered photon emerges from the collision in a new direction and with reduced energy and increased wavelength. The change in wavelength, $\lambda' - \lambda$ commonly referred to as the Compton shift given by equation (2.5).

$$\lambda' - \lambda = \frac{h}{m_o c}(1 - \cos\theta) = 0.024264\ (1 - \cos\theta)\ \text{Å} \qquad (2.5)$$

It is notable that the change in wavelength (and decrease in energy) of the photon is determined only by the scattering angle. The term $h/m_o c^2$, often called the Compton wavelength, has the value 2.4264×10^{-10} cm (Martin, 2006).

At low energies, a large fraction of the incident energy is carried away by the scattered photons, but as the energy increases, a greater energy fraction is transferred to the recoil electron. At energies well beyond diagnostic imaging, a photon of $\sim$1.5 MeV, for example, shares energy equally between the scattered photon and local energy absorption (Seibert et al, 2005). This is shown in Figure 2.2.

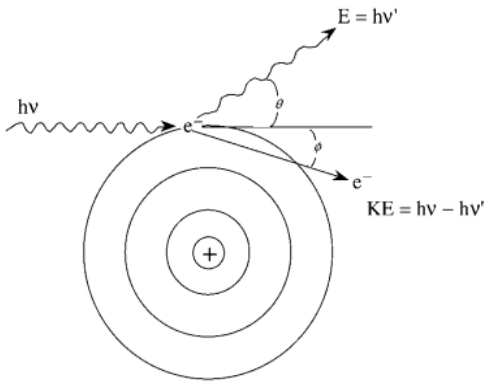

Figure 2.2: Compton scattering with a "free" electron.

Energy transfer to the recoiling electron is the most important consequence of Compton interactions since it will be absorbed locally to produce radiation dose. The Compton interaction coefficient σ consists of two components: $\sigma = \sigma_a + \sigma_s$

where σ is the total Compton interaction coefficient, σ_a is the Compton absorption coefficient for photon energy lost by collisions with electrons, and σ_s is the loss of energy due to the scattering of photons out of the beam. The Compton interaction coefficient is determined by electron density which is directly related to Z and inversely proportional to E given by equation (2.6)(Martin, 2006).

$$\sigma \cong k \times \frac{Z}{E} \qquad (2.6)$$

Where k is a constant.

2.1.3.3 Pair Production

Pair production can occur when the incident X-ray or γ-ray photon has energy greater than 1.02 MeV, which represents the rest mass energy equivalent of 2 electrons (Knoll, 2000). The interaction of the incident photon with the electric field of the nucleus results in the production of an electron (e^-)–positron (e^+) pair, with any photon energy in excess of $1.02 MeV$ being transferred to the kinetic energy of the e^-/e^+ pair equally. Interestingly, ionization of the atom does not occur, although charged particles are formed and their kinetic energy can result in subsequent ionization within the local area. Once the positron expends its kinetic energy, it will combine with any available electron and produce annihilation radiation, resulting from the conversion of the rest mass energies of the e^-/e^+ pair into (nearly) oppositely directed $511-keV$ photons (Seibert et al, 2005).

Pair production is a classic example of Einstein's special theory of relativity in which the pure energy of the photon is converted into two electron masses, and since energy is conserved the positron and electron share the energy left over $(h\upsilon - 1.022)$ after the electron masses have been formed. This remaining energy appears as kinetic energy of the e^+ and e^- pair, but is not shared equally. The positively charged nucleus repels the positively charged positron which provides an extra "kick" while the negatron is attracted and thus slowed down with a decrease in its kinetic energy. Because of these circumstances, the positron should receive a maximum of about $0.0075Z$ more kinetic energy than the average negatron. The slight difference in energy shared by the positron and the electron in pair production interactions is of little consequence to radiation dosimetry or detection since the available energy,

$(h\upsilon - 1.022)MeV$, will be absorbed in the medium with the same average result regardless of how it is shared (Martin, 2006).

Pair production interactions are also accompanied by the emission of two annihilation photons of $0.511MeV$ each, which are also shown in Figure 2.3.

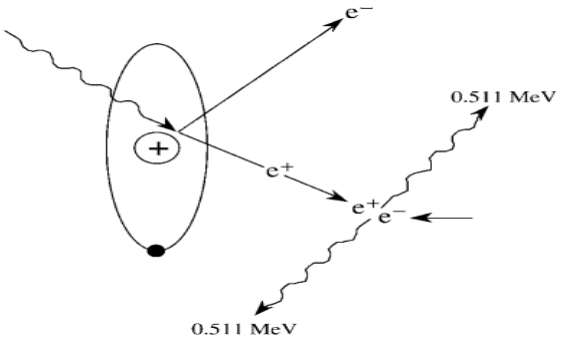

Figure 2.3: Pair production.

The positron will exist as a separate particle as long as it has momentum and kinetic energy. However, when it has been fully absorbed, being antimatter in a matter world, it will interact with a negatively charged electron forming for a brief moment a "neutral particle" of "positronium" which then vanishes yielding two $0.511MeV$ photons; i.e., mass becomes energy. The absorption of high-energy photons thus yields a complex pattern of energy emission and absorption in which the pure energy of the photon produces an electron and a positron which deposit $(h\upsilon - 1.022)MeV$ of kinetic energy along a path of ionization, followed in turn by positron annihilation with a free electron to convert mass back into energy. The absorption of a high-energy photon by pair production thus yields two new photons of $0.511MeV$ which may or may not interact in the medium and an intermediate pair of electron masses which almost certainly do.

Since pair production is an electromagnetic interaction, it can take place only in the vicinity of a Coulomb field. At most γ-ray energies of interest, this is the field of the nucleus, not the surrounding electrons (Lamash et al, 2001).

The pair production interaction coefficient κ is proportional to the square of the atomic number Z for photons with energy greater than $(2\times 0.511)MeV$ (the energy required to form an electron–positron pair) given by equation (2.7).

$$\kappa \cong k \times Z^2 (E - 1.022) \qquad (2.7)$$

Where *k* is a constant, Z is the atomic number and E is the photon energy in MeV (Martin, 2006).

2.1.4 Attenuation Coefficients

The total cross-section per atom for γ-ray interaction is the sum of the cross-sections for the photoelectric effect, pair production, and Compton scattering by equation (2.8) (Lamash et al, 2001).

$$\sigma = \sigma_{pe} + \sigma_{pp} + \sigma_c \qquad (2.8)$$

A macroscopic cross-section can also be defined by multiplying σ in Equation (2.8) by the atom density N. By tradition, such macroscopic γ-ray cross-sections are called attenuation coefficients and are denoted by the symbol μ. This is given by equation (2.9).

$$\mu = N\sigma = \mu_{pe} + \mu_{pp} + \mu_c \qquad (2.9)$$

(Lamash et al, 2001).

Where μ is the total attenuation coefficient and μ_{pe}, μ_{pp} *and* μ_c are the attenuation coefficients for the three interaction processes. The various $\mu's$ have units of cm^{-1}. It is also convenient to define the quantity μ/ρ, which is called the mass attenuation coefficient, where ρ is the physical density. This is given by equation (2.10).

$$\frac{\mu}{\rho} = \frac{\mu_{pe}}{\rho} + \frac{\mu_{pp}}{\rho} + \frac{\mu_c}{\rho}. \qquad (2.10)$$

(Lamash et al, 2001).

2.2 Dosimetric Principles

Technically radiation protection is the measure to reduce exposure to radiation, and radiation dosimetry is the measurement of radiation doses. Radiation measurements and investigations of radiation effects require various specifications of the radiation field at the point of interest. Radiation dosimetry deals with methods for a quantitative determination of energy deposited in a given medium by directly or indirectly ionizing radiations (IAEA, 2005).

A radiation dosimeter is a device, instrument or system that measures or evaluates, either directly or indirectly, the quantities exposure, kerma, absorbed dose or equivalent dose, or their time derivatives (rates), or related quantities of ionizing radiation. A dosimeter along with its reader is referred to as a dosimetry system (IAEA, 2005).

Measurement of a dosimetric quantity is the process of finding the value of the quantity experimentally using dosimetry systems. The result of a measurement is the value of a dosimetric quantity expressed as the product of a numerical value and an appropriate unit (IAEA, 2005).

A number of quantities and units have been defined for describing the radiation beam, and the most commonly used dosimetric quantities and their units are defined below. A simplified discussion of Bragg-Gray cavity theory, the theory that deals with calculating the response of a dosimeter in a medium, is also given (IAEA, 2005).

2.2.1 Photon Fluence and Energy Fluence

The following quantities are used to describe a monoenergetic ionizing radiation beam: particle fluence, energy fluence, particle fluence rate and energy fluence rate. These quantities are usually used to describe photon beams and may also be used in describing charged particle beams.

The particle fluence Φ is the quotient dN by dA given by equation (2.11).

$$\Phi = \frac{dN}{dA} \qquad (2.11)$$

Where dN is the number of particles incident on a sphere of cross-sectional area dA.

The unit of particle fluence is m^{-2}. The use of a sphere of cross-sectional area dA expresses in the simplest manner the fact that one considers an area dA perpendicular to the direction of each particle and hence that particle fluence is independent of the incident angle of the radiation.

The energy fluence Ψ is the quotient of dE by dA given by equation (2.12).

$$\Psi = \frac{dE}{dA} \qquad (2.12)$$

Where dE is the radiant energy incident on a sphere of cross-sectional area dA.

The unit of energy fluence is Jm^{-2}. Energy fluence can be calculated from particle fluence by using equation (2.13).

$$\Psi = (dN/dA) \times E = \Phi E \qquad (2.13)$$

Where E is the energy of the particle and dN represents the number of particles with energy E.

The particle fluence rate $\dot{\Phi}$ is the quotient of $d\Phi$ by dt given by equation (2.14).

$$\dot{\Phi} = \frac{d\Phi}{dt} \qquad (2.14)$$

Where $d\Phi$ is the increment of the fluence in time interval dt.

The unit of particle fluence rate is $m^{-2}s^{-1}$. The energy fluence rate (also referred to as intensity) is the quotient of $d\Psi$ by dt given by equation (2.15).

$$\dot{\Psi} = \frac{d\Psi}{dt} \qquad (2.15)$$

Where $d\Psi$ is the increment of the energy fluence in the time interval dt. The unit of energy fluence rate is W/m^2 or $Jm^{-2}s^{-1}$ (IAEA, 2005).

2.2.2 Exposure Measurement

The term exposure is used to describe the quantity of ionization produced when X-rays or gamma rays interact in air because it can be conveniently measured directly by collecting the electric charge, whereas that which occurs in a person cannot be (Martin, 2006).

When the ion chamber is exposed to X-radiation or to gamma radiation, the ionization, which is produced in the measuring cavity as a result of interactions between photons and the wall, discharges the condenser, thereby decreasing the potential of the anode. This decrease in the anode voltage is directly proportional to the ionization produced in the cavity, which in turn is directly proportional to the radiation exposure (Cember et al, 2009).

Exposure X is the quotient of dQ by dm given by equation (2.16).

$$X = \frac{dQ}{dm} \qquad (2.16)$$

Where dQ is the absolute value of the total charge of the ions of one sign produced in air when all the electrons and positrons liberated or created by photons in mass dm of air are completely stopped in air. The unit of exposure is coulomb per kilogram (C/kg) (IAEA, 2005).

2.2.3 Kerma

Kerma is the kinetic energy released per unit mass. It is a non-stochastic quantity applicable to indirectly ionizing radiations. It quantifies the average amount of energy transferred from indirectly ionizing radiation to directly ionizing radiation without concern as to what happens after this transfer (IAEA, 2005).

In the case of indirectly ionizing radiation, such as X-rays, gamma rays, and fast neutrons, we are sometimes interested in the initial kinetic energy of the primary ionizing particles (the photoelectrons, Compton electrons, or positron–negatron pairs in the case of photon radiation and the scattered nuclei in the case of fast neutrons) that result from the interaction of the incident radiation with a unit mass of interacting

medium. This quantity of transferred energy is called the kerma, K, and is measured in joules per kilogram(J/kg). Although kerma and dose are both measured in the same units, they are different quantities. The kerma is a measure of all the energy transferred from the uncharged particle (photon or neutron) to primary ionizing particles per unit mass, whereas absorbed dose is a measure of the energy absorbed per unit mass (Cember, 2009).

Not all the energy transferred to the primary ionizing particles in a given volume of material may be absorbed in that volume. Some of this energy may leave that volume and be absorbed. This could result from bremsstrahlung or annihilation radiation which is generated by the primary ionizing particles, but which leave the volume element without further interactions within that volume. It may also be the result of failure to attain electronic equilibrium within the volume element under consideration. In a large medium, where electronic equilibrium exists and where we have insignificant energy loss by bremsstrahlung, kerma is equal to absorbed dose (Cember, 2009).

The energy of photons is imparted to matter in a two stage process. In the first stage, the photon radiation transfers energy to the secondary charged particles (electrons) through various photon interactions (the photoelectric effect, the Compton effect, pair production, etc.). In the second stage, the charged particle transfers energy to the medium through atomic excitations and ionizations (IAEA, 2005).

The kerma is defined as the quotient of dE_{tr} by dm given by equation (2.17).

$$K = \frac{dE_{tr}}{dm} \tag{2.17}$$

where dE_{tr} is the sum of the initial kinetic energies of all the charged ionizing particles (electrons and positrons) liberated by uncharged particles (photons) in a material of mass dm (Khan, 2003).

A major part of the initial kinetic energy of electrons in low atomic number materials (e.g., air, water, soft tissue) is expended by inelastic collisions (ionization and excitation) with atomic electrons. Only a small part is expended in the radiative collisions with atomic nuclei (bremsstrahlung). Kerma can thus be divided into two parts as given by equation (2.18).

$$K = K^{col} + K^{rad} \tag{2.18}$$

Where K^{col} and K^{rad} are the collision and the radiation parts of kerma, respectively (Khan, 2003).

The absorbed dose is related to the stochastic quantity energy imparted. The absorbed dose is defined as the mean energy $\bar{\varepsilon}$ imparted by ionizing radiation to matter of mass m in a finite volume V given by equation (2.19).

$$D = \frac{d\bar{\varepsilon}}{dm} \tag{2.19}$$

The energy imparted $\bar{\varepsilon}$ is the sum of all the energy entering the volume ofinterest minus all the energy leaving the volume, taking into account any mass–energy conversion within the volume. Pair production, for example, decreases the energy by 1.022 MeV, while electron–positron annihilation increases the energy by the same amount.

Because electrons travel in the medium and deposit energy along their tracks, this absorption of energy does not take place at the same location as the transfer of

energy described by kerma. The unit of absorbed dose is joule per kilogram (IAEA, 2005).

2.2.4 Stopping Power

Stopping powers are widely used in radiation dosimetry, but they are rarely measured and must be calculated from theory. For electrons and positrons the Bethe theory is used to calculate stopping powers (IAEA, 2005).

The linear stopping power is defined as the expectation value of the rate of energy loss per unit path length (dE/dx) of the charged particle. The mass stopping power is defined as the linear stopping power divided by the density of the absorbing medium. Typical units for the linear and mass stopping powers are MeV/cm and $MeVcm^2/g$, respectively (IAEA, 2005).

Two types of stopping power are known: collision (ionization), resulting from interactions of charged particles with atomic orbital electrons; and radiative, resulting from interactions of charged particles with atomic nuclei (IAEA, 2005).

The total mass stopping power is the sum of the collision mass stopping power and the radiative mass stopping power (IAEA, 2005).

2.2.5 Absorbed Dose Measurement: Bragg–Gray Principle

According to the Bragg–Gray principle, the amount of ionization produced in a small gas-filled cavity surrounded by a solid absorbing medium is proportional to the energy absorbed by the solid. Implicit in the practical application of this principle is that the gas cavity be small enough relative to the mass of the solid absorber to

leave the angular and velocity distributions of the primary electrons unchanged. This requirement is fulfilled if the primary electrons lose only a very small fraction of their energy in traversing the gas-filled cavity. If the cavity is surrounded by a solid medium of proper thickness to establish electronic equilibrium, then the energy absorbed per unit mass of wall, dE_m/dM_m is related to the energy absorbed per unit mass of gas in the cavity, dE_g/dM_g , by equation (2.20).

$$\frac{dE_m}{dM_m} = \frac{S_m}{S_g} \times \frac{dE_g}{dM_g} \qquad (2.20)$$

where S_m is the mass stopping power of the wall material and S_g is the mass stopping power of the gas.

Since the ionization per unit mass of gas is a direct measure of dE_g/dM_g , Equation (2.20) can be rewritten as equation (2.21).

$$\frac{dE_m}{dM_m} = \rho_m \times \omega \times J \qquad (2.21)$$

where

$\rho_m = S_m/S_g$,

ω = the mean energy dissipated in the production of an ion pair in the gas, and

J = the number of ion pairs per unit mass of gas.

Using the appropriate equations for stopping power given above, we can compute ρ_m for electrons of any given energy. For those cases where the gas in the cavity is the same substance as the chamber wall, such as methane and paraffin, ρ_m is

equal to unity. For gamma radiation, the problem of evaluating ρ_m is more difficult. The relative fraction of the gamma rays that will interact by each of the competing mechanisms, as well as the spectral distribution of the primary electrons (Compton, photoelectric, and pair-produced electrons) must be considered, and a mean value for relative stopping power must be determined. For air, ω, the mean energy loss for the production of an ion pair in air, has a value of $34eV$. To determine the radiation absorbed dose, it is necessary only to measure the ionization J per unit mass of gas (Cember, 2009).

Although the cavity size is not explicitly taken into account in the Bragg–Gray cavity theory, the fulfilment of the two Bragg–Gray conditions will depend on the cavity size, which is based on the range of the electrons in the cavity medium, the cavity medium and the electron energy. A cavity that qualifies as a Bragg–Gray cavity for high energy photon beams, for example, may not behave as a Bragg–Gray cavity in a medium energy or low energy X- ray beam (IAEA, 2005).

2.3 Basis of Radiation Protection

The development of a radiation technology left in its trail occupational casualties—physicists, radiologists, radiation chemists—researchers who investigated the properties and uses of these energetic radiations without appreciating their capacity for destructive effects in living matter. But society soon recognized the harm that energetic radiations could cause when exposure was uncontrolled, and it has worked diligently since to further the understanding of the biological effects of radiation and to establish acceptable limits of exposure (Shapiro, 2002).

Governments realized that effective measures were necessary to protect radiation workers and the public from excessive exposure to radiation. This has necessitated the enactment of extensive legislation, the establishment of regulatory bodies and authorisations mechanisms, the setting of standards of radiation exposure, and the requirement for the training of occupationally exposed workers to conform to acceptable safety culture within practices and sources within practices (Shapiro, 2002).

2.3.1 Deterministic and Stochastic Effects

Shortly after the discoveries of X-rays and radioactivity, it was recognized that excessive exposure to radiation might cause some visible or observable detriments to health. These effects, now called deterministic, occur when radiation kills a large number of important cells in a tissue. The probability of causing such harm is essentially zero at small doses, but above a certain threshold dose it jumps suddenly to unity. The severity of the inflicted harm also increases with the radiation dose (Sabol et al, 1995).

Later, in the early nineteen twenties, another effect on health was noticed-cancer, induced by radiation exposure. The initiation of malignant conditions is related to the modification of irradiated cells rather than their destruction. This kind of effect is characterized by long latent periods (even several decades) and random occurrences, the probability of which depends on the total dose received by an individual. The resulting biological harm is statistical in nature so it termed stochastic effect. These effects may be manifested in the exposed person (somatic effects) or they may affect his/her progeny (genetic effects) (Sabol et al, 1995).

2.4 Uncertainty of Measurements

Radioactive decay is a random process. Consequently, any measurement based on observing the radiation emitted in nuclear decay is subject to some degree of statistical fluctuation. These inherent fluctuations represent an unavoidable source of uncertainly in all nuclear measurements and often can be the predominant source of imprecision or error (Knoll, 2000).

The uncertainty associated with measurement is a parameter that characterises the dispersion of the values that could reasonably be attributed to the measurand. This parameter is normally an estimated standard deviation. It has no known sign and is usually assumed to be symmetrical. Uncertainties of measurement in this study were calculated and expressed in accordance with the BIPM, IEC, ISO, IUPAP, OIML document (International Organisation for Standardisation, 1993).

Two types of standard uncertainties, type A and type B are considered in this work. The type A standard uncertainty is obtained by statistical means. In principle, increasing the number of individual readings could reduce this uncertainty contributor. There are many sources of measurement uncertainty that cannot be estimated by repeated measurements. They are called type B uncertainty. These include not only unknown, although suspected, influences on the measurement process, but also little known effects of influence quantities such as temperature and pressure for air kerma measurements, application of correction factors, etc(IAEA 2000).

2.4.1 Type A Standard Uncertainties

In a series of n measurements, with observed values x_i, the best estimate of the quantity x is usually given by the arithmetic mean value, $\bar{x}$ given by equation (2.22).

$$\bar{x} = \frac{1}{n}\sum_{i=1}^{n} x_i \qquad (2.22)$$

The fact that the readings vary indicates the presence of randomly varying influences, and the point of taking the mean value is to estimate what the reading would be in the absence of these random variations.

The scatter of the n measured values x_i, around their mean $\bar{x}$ can be characterized by the standard deviation which is estimated using equation (2.23).

$$s(x) = \sqrt{\frac{1}{n-1}\sum_{i=1}^{n}(x_i - \bar{x})^2} \qquad (2.23)$$

This expression is not defined in the case $n = 1$, for the simple reason that no conclusion can be drawn about the width of the distribution $p(x)$ when only one reading is taken. That is why one divides by $n-1$ rather than by n (IAEA, 2000).

The standard deviation of the mean $s(\bar{x})$ is given by equation (2.24).

$$s(\bar{x}) = \frac{s(x)}{\sqrt{n}} = \sqrt{\frac{1}{n(n-1)}\sum_{i=1}^{n}(x_i - \bar{x})^2} \qquad (2.24)$$

The standard uncertainty of type A, denoted here by u_A, is identified with the standard deviation of the mean value given by equation (2.25).

$$u_A = s(\bar{x}) \qquad (2.25)$$

The number of degrees of freedom associated with this standard uncertainty is given by equation (2.26).

$$\upsilon_x = n - 1 \qquad (2.26)$$

2.4.2 Type B Standard Uncertainties

There are many sources of measurement uncertainty that cannot be estimated by repeated measurements. They are called type B uncertainties. The evaluation of type B uncertainties are based on scientific judgement using all of the relevant information available, which includes previous measurement data; experience with, or general knowledge of the behaviour and property of relevant materials and instruments; manufacturer's specifications; data provided in calibration and other reports and uncertainties assigned to reference data taken from handbooks (IAEA, 2000; IAEA, 2009).

Type B uncertainties must be estimated so that they correspond to standard deviations; they are called type B standard uncertainties. It is often helpful to assume that these uncertainties have a probability distribution which corresponds to some easily recognizable shape. It is sometimes assumed, mainly for the sake of simplicity, that type B uncertainties can be described by a rectangular probability density, that is that they have equal probability anywhere within the given maximum limits -M and +M. It can be shown that with this assumption, the type B standard uncertainty u_B is given by equation (2.27).

$$u_B = \frac{M}{\sqrt{3}} \qquad (2.27)$$

Alternatively, if the assumed distribution is triangular (with the same limits), we are led to the relation in equation (2.28).

$$u_B = \frac{M}{\sqrt{6}} \tag{2.28}$$

Another assumption is that type B uncertainties have a distribution that is approximately Gaussian (normal). On this assumption, the type B standard uncertainty can be derived by first estimating some limits ±L and then dividing that limit by a suitable number. If, for example, the experimenter is fairly sure of the limit L, it can be considered to correspond approximately to a 95% confidence limit, whereas if the experimenter is almost certain, it may be taken to correspond approximately to a99% confidence limit (IAEA, 2000; IAEA, 2009; European Co-operation for Accreditation, 1999).

. Thus, the type B standard uncertaintyu_B can be obtained from equation (2.29).

$$u_B = \frac{L}{k} \tag{2.29}$$

Where $k = 2$ if the experimenter is fairly sure and $k = 3$ if the experimenter is almost certain of his or her estimated limits $\pm L$. These relations correspond to the properties of a Gaussian distribution and it is usually not worthwhile to apply divisors other than 2 or 3 because of the approximate nature of the estimation.

There are thus no rigid rules for estimating type B standard uncertainties. The experimenter should use his or her best knowledge and experience and, whichever method is applied, provide estimates that can be used as if they were standard deviations. There is hardly ever any meaning in estimating type B uncertainties to more than one significant figure, and certainly never to more than two (IAEA 2000).

2.4.3 Combined and Expanded Uncertainties

Since Type A and Type B uncertainties are both estimated standard deviations, they are combined by using the statistical rules for combining variances (which are squares of standard deviations). If u_A and u_B are type A and type B standard uncertainties of a quantity, respectively, the combined standard uncertainty of that quantity is given by equation (2.30).

$$u_C = \sqrt{u_A^{\,2} + u_B^{\,2}} \qquad (2.30)$$

The combined standard uncertainty thus still has the character of a standard deviation. If, in addition, it is believed to have a Gaussian probability density, then the standard deviation corresponds to a confidence limit of about 68%. Therefore, it is often felt desirable to multiply the combined standard uncertainty by a suitable factor, called the coverage factor k, to yield an expanded uncertainty. Values of the coverage factor of $k = 2$ or 3 corresponding to confidence limits of about 95% or 99%. The approximate nature of uncertainty estimates, in particular for Type B, makes it doubtful that more than one significant figure is ever justified in choosing the coverage factor. In any case, the numerical value taken for the coverage factor should be clearly indicated (IAEA, 2000; IAEA, 2009; Lewis et al, 2003;European Co-operation for Accreditation, 1999).

2.5 International Guidance

The International Organization for Standardization (ISO), incooperation with the International Electrotechnical Commission (IEC), has developed a standard (ISO/IEC 17025) entitled General Requirements for the Competence of Testing and

Calibration Laboratories, which describes the requirements a laboratory must meet to receive ISO certification (IAEA, 2009; ISO, 2005).

A key aspect of ISO/IEC 17025 is the establishment of a quality management system within the calibration laboratory. ISO defines the quality management system as "the quality, administrative and technical systems that govern the operations of a laboratory" and it can be thought of as the system put in place to manage quality (IAEA, 2009; ISO, 2005).

The International Organization for Standardization, (1996) describes the characteristics and production methods for establishing X-ray reference radiation. The standard specifies the characteristics of filtered X-ray radiation in terms of tube voltage, mean energy, resolution and HVL. Table 2.1 show these specifications for the qualities included in this study (IAEA, 2000; Bohm et al,1999).

Table 2.1: Characteristics of X-ray qualities of the narrow spectrum

Radiation quality	Mean energy $\bar{E}$(keV)	Resolution Re (%)	Tube potential (kV)	Additional filtration (mm)				First HVL (mm)	Second HVL (mm)
				Pb	Sn	Cu	Al		
N-30	24	32	30				4.0	1.15 Al	1.30 Al
N-40	33	30	40			0.21		0.084 Cu	0.091 Cu
N-60	48	36	60			0.6		0.24 Cu	0.26 Cu
N-80	65	32	80			2.0		0.58 Cu	0.62 Cu
N-100	83	28	100			5.0		1.11 Cu	1.17 Cu
N-150	118	37	150		2.5			2.36 Cu	2.47 Cu
N-200	164	30	200	1.0	3.0	2.0		3.99 Cu	4.05 Cu
N-250	208	28	250	3.0	2.0			5.19 Cu	5.23 Cu

ISO (1996) provides that, for the narrow-spectrum series, the mean energy shall be within $\pm 3\%$, the resolution within $\pm 10\%$, and the tube potential within $\pm 2\%$ of the values specified in the standard. The inherent filtration of the X-ray tubes is 1 mm Be (IAEA, 2000; Bohm et al,1999).

ISO (1999) defines the conversion coefficients from air-kerma to ambient dose equivalent, directional dose equivalent and personal dose equivalent, both for mono-energetic radiation and for qualities included in the different series (IAEA, 2000; Bohm et al,1999; European Co-operation for Accreditation, 1999). This is shown in Tables 2.2 and 2.3 for narrow spectrum series and for radiation of normal incidence.

Table 2.2: X-ray reference radiation conversion coefficients

Radiation quality	Mean energy $\bar{E}(keV)$	Conversion coefficient, h $H^*(10)/K_a\ (SvGy^{-1})$
N-60	48	1.59
N-80	65	1.73
N-100	83	1.71
N-150	118	1.58
N-200	164	1.46
N-250	208	1.39

Table 2.3: Conversion coefficient for ^{137}Cs source

Radiation quality	Energy of radiation (MeV)	Half-life (d)	Air kerma rate constant $(\mu Gyh^{-1}m^2MBq^{-1})$	Conversion coefficient for normal incidence $H^*(10)/K_a\ (SvGy^{-1})$
S-Cs	0.6616	11050	0.079	1.20

CHAPTER THREE

MATERIALS AND METHODS

A description of the materials and methods employed in the experimental study is presented in this chapter.

3.1 Description of irradiation facility

The experimental study was carried out at the SSDL facility at GAEC. This facility contains a calibration bunker and a control room. The calibration bunker is constructed with a 40 cm thickness of concrete, 8 meters wide and 12 meters long. The main radiation sources include a constant potential x-ray system with a 320 kV tube and a collimated ^{137}Cs gamma irradiator. Currently, only the collimated ^{137}Cs source is used for calibration of personnel dosimeters and radiation protection instrument. The materials and equipment used in this study also include the SSDL reference instrument, barometer, thermometer, hygrometer, survey meters, closed circuit television camera **(**CCTV), calibration bench with telescopic and laser alignment systems, retort stand, absorbers of aluminium (Al) and copper (Cu), TLD cards and ICRU slab phantom.

3.1.1 X-ray unit

The SSDL employs a constant voltage type generator as a source of the high potential applied to the X-ray tube, which gives high output stability. The X-ray unit was manufactured by Philips and it has a generating potential in the range of 60 kV to 320 kV. The serial number is 90106004. The X-ray machine is housed in a small enclosure with no movement of the x-ray tube as shown in Plate 3.6.

3.1.2 Collimated ^{137}Cs Gamma ray unit

The source used for calibration at the SSDL is the ^{137}Cs panoramic source from the irradiator USA.DOT-7A type A produced by J. L Shepherd and Associates. A lead block mould is used to collimate the panoramic ^{137}Cs source. This is to collimate the panoramic isotropic beam into narrow beam geometry to enhance the calibration of personnel dosimeters and radiation survey meters and further reduces scattered radiations due to backscatter and transmission through the biological shield. The lead-block collimator is made of pure lead, moulded into a block with a length of 19.1 cm, a width of 15.9 cm and height of 20.1 cm. It has two drilled holes, one in front of the block which is 4.7 cm in diameter that allow γ-ray photons to emerge during irradiation process. The other hole is on top of the block which is 3.2 cm in diameter and serves as a support for the protruded panoramic tube. The collimator setting is fixed throughout the calibration procedure. Plate 3.8 shows the setup of the 22.2 GBq ^{137}Cs source with the lead block collimator in place.

It has a storage lead case which houses the radioactive source when at storage position. The source is connected to a nitrogen gas cylinder which helps to move the source to the irradiation position during irradiation. If source does not come to full position errors will be introduced. The source is moved to a fully shielded position when radiation is switched 'off'.

3.1.3 SSDL Reference Instrument

The SSDL reference instrument consists of ionisation chamber and electrometer. The ionization chamber is a spherical detector and is manufactured by PTW Freiburg with model/type LS-01 and serial number 227. It has a measuring volume of 1000 cm^{3}and is mostly air-filled and unsealed. It is used principally to

monitor beta, gamma, and X radiation, their sensitivity depends on the volume and pressure of the gas and on the associated electronic readout components (Tuner, 2007). The electrometer is the charge measuring device and is also manufactured by PTW Freiburg with model/type UNIDOS and serial number 20243. It is connected to the ionisation chamber through a PTW M-System, BNT or TNC triax connectors. It displays the charge value in picocoulomb or nanocoulomb. The ionisation chamber together with the electrometer was calibrated at the IAEA Primary Standards Laboratory in Vienna (radiation protection level calibration) for ^{137}Cs, ^{60}Co gamma and ISO 4037 X-ray qualities (narrow-spectrum series). This standard chamber with the electrometer was used to establish the dose profile at the SSDL in Ghana in terms of air kerma free-in-air (Carlsson et al,1996). In the process, the laser alignment systems were used to check that the chamber is correctly positioned at the desired source-detector distance. Ionization chambers for radiation monitoring are air filled and unsealed.

Instruments, which are used to measure directional dose equivalent and personal dose equivalent, shall have a defined directional response. Examples of detectors that can measure the ambient dose equivalent are ionisation chambers and GM tubes. Also passive detectors, like TLDs, can be used (Carlsson et al, 1996).

3.1.4 Barometer

For measuring the air pressure, a calibrated barometer shown in Plate 3.1 was used for the study.

Plate 3.1: Barometer

The barometer is located in the same room as the ionization chamber at about the same height as the chamber. The pressure was measured at nearly the same time as the chamber reading is obtained.

3.1.5 Digital thermometer

For measuring the ambient temperature, a calibrated digital thermometer serial number TL 1291 DKD-K-50401 was used during the experiment as shown in Plate 3.2.

Plate 3.2: Digital thermometer

The measuring range is from -50 ^{0}C to +200^{0}C. It is positioned near the ionization chamber without disturbing the radiation field. The temperature was measured at nearly the same time as the chamber reading is obtained.

3.1.6 Hygrometer

The hygrometer serial number 48/12 was used to determine the relative humidity, which influences several parameters such as the air density, the average energy for producing an ion pair (W value) and the mass stopping power for electrons. This is shown in Plate 3.3.

Plate 3.3: Hygrometer

If the relative humidity varies between 20% and 70% at the usual operating temperatures, the response of an ionization chamber changes by less than 0.1% as a result of the combined effect of these three parameters. So usually no humidity correction is applied (IAEA, 2008).

3.1.7 Closed Circuit Television Camera (CCTV)

The camera is an outdoor IP44 weather proof CM OS camera with a night vision up to 15 m. It is connected by an 18 meter cable to a monitor. The monitor has a 7' LCD screen with a resolution of 480 (H) x 240 (V). It has 3 channel AV input with 1 x AV output with a DC input voltage of 12 volts. The CCTV camera was mounted alongside the ionisation chamber to view the experimental set up from the control room during irradiation. The camera was also used to capture the readings of

the instrument under calibration and was indicated on the monitor positioned in the control room.

3.1.8 Gamma Survey Meters

Plate 3.4shows two gamma survey meters, RADEYE G-10 with serial number 42506/76-F and RADEYE PRD with serial number 42506/71-F used during the experimental work and when entering the calibration bunger to monitor the ambient dose rates while inside.

Plate 3.4: Gamma survey meters

These radiation detection, dose and dose rate monitors are highly sensitive and rugged measuring devices to detect and localize radiation sources and to measure the dose rate of gamma radiation (Chidal et al 2008).

3.1.9 Control Room Set up

In the control room is located the X-ray control unit, the X-ray fast shutter control unit, the ^{137}Cscontrol unit, the electrometer, the *HVL* control unit, the filter wheel control and the monitor as shown in Plate 3.5.

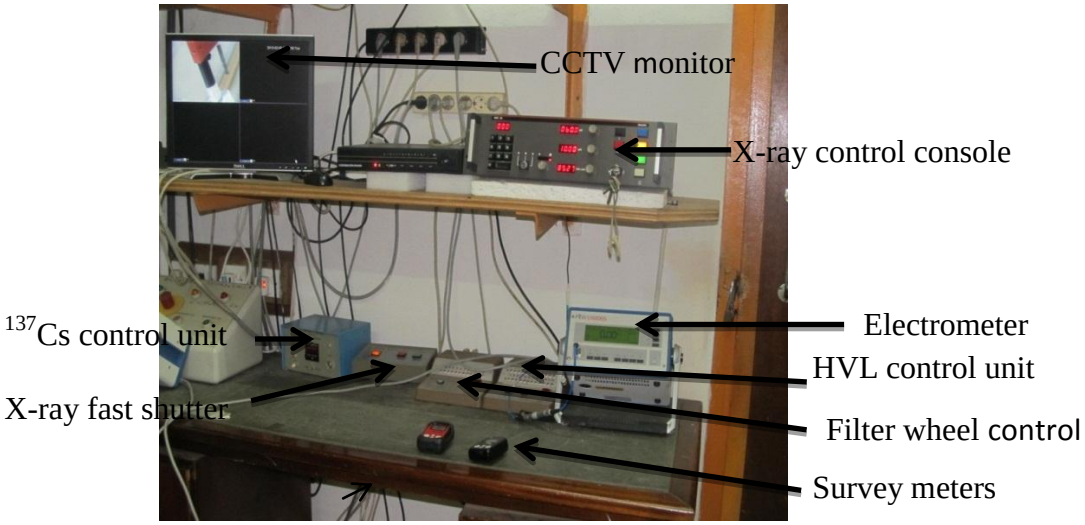

Plate 3.5: Control room set up.

The exposures are carried out from the control room and the monitor is used to view the experimental set up during calibration of equipment (survey meters). The charges measured by the ionisation chamber are collected by the electrometer.

3.2 Methods

This section describes in details the methods employed in the experimental study.

3.2.1 Verification of X-ray Qualities

The radiation quality of an X-ray beam is normally characterized by tube potential, total filtration and first half value layer (IAEA, 2008). These qualities are given as standards at the various energies. To verify these qualities *HVL* was determined for X-ray energies of 60 kV to 250 kV. Plate 3.6 describes the setup for the measurement of *HVL* in the calibration bunker.

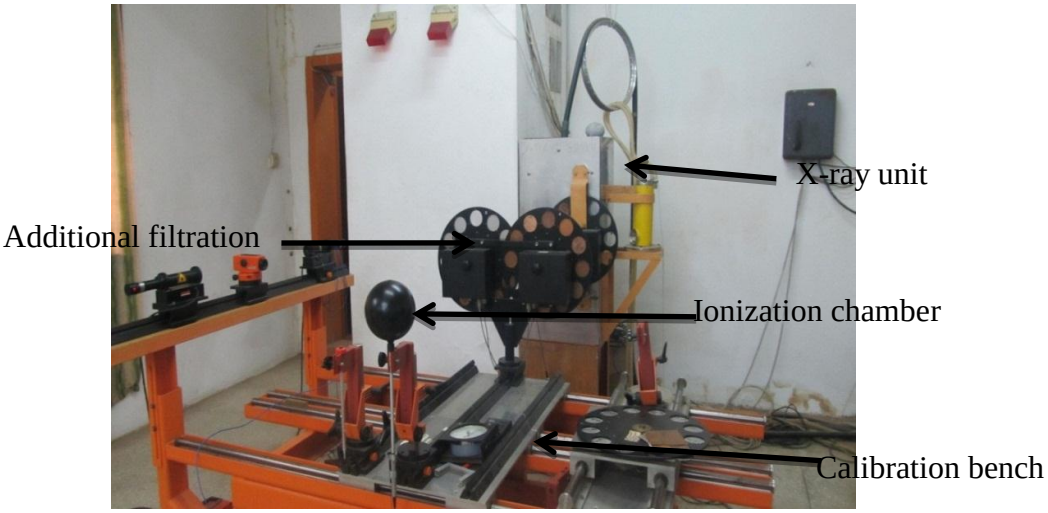

Plate 3.6: Experimental set-up for *HVL* measurement

The determination of HVL involved the successive measurement of air kerma at a point in the narrow beam, as the thickness of the attenuating material in the beam was increased. The *HVL* of the X-ray beam was obtained by measuring the exposure rate of the x-ray machine for a series of different attenuators placed in the beam. The kV and mA of the tube are kept constant during the measurement. *HVL* of X-ray

beam is the thickness of material (in this case aluminium or copper) necessary to reduce incident X-ray intensity by one half and is determined by measuring X-ray transmission as function of attenuator thickness (Seibert et al, 2005). The *HVL* was measured under good geometry conditions with the SSDL reference standard ionization chamber and a set of known filter thicknesses (typically) of aluminium (Charlie, 2009).

If the *HVL* is in agreement with ISO4037 values the dose profiling was done. For *HVL* that do not agree with ISO value added filtration was introduced to modify the beam to obtain *HVL* for that energy.

The absorber was positioned midway between the monitor chamber and the measuring chamber shown in Plate 3.6 so as to minimize radiation scattering into either.

The field size should be the smallest available that irradiates the sensitive volume of the chamber completely and reasonably uniformly. Each absorber must be substantially larger than the X-ray beam so that it intercepts the beam completely (IAEA, 2009).

For X-ray qualities of 100 kV and above, absorbers of copper are used; copper sheets of known thickness between 0.1 mm and 5 mm are generally required. For qualities below 100 kV, aluminium is better suited (copper filters would be too thin and fragile) and aluminium sheets of thickness between 0.02 mm and 5 mm are required. The metals should have a purity of at least 99.9%. The absorbers should have adequately uniform thickness and should be as homogeneous as possible and without visible pinholes, cracks, macroscopic grains (IAEA, 2009).

For a given generating potential and filter combination, the measured HVL should agree with the expected value within about 2%, which is a typical uncertainty for a measurement of HVL (a larger deviation is acceptable below 20 kV). If this is not the case, the thickness and density of the filters and the absorbers used to measure HVL should be verified. If these are correct, the filtration should be adjusted to obtain the desired HVL (within 2%) (IAEA, 2009).

The general radiation transmission and shielding equation is given by the equation

$$I = I_o e^{-\mu x} \qquad (3.1)$$

where

I is the radiation intensity after transmitting through the medium,

I_o is the initial radiation before transmission through the material,

x is the absorber thickness in cm and

μ is the linear attenuation coefficient in cm^{-1}(Smith, 2000; Knoll,1999).

The HVL equation is given by

$$HVL = \frac{\ln 2}{\mu} \qquad (3.2)$$

3.2.1.1 Conditioning of X-ray Tube

The X-ray tube was first conditioned before the start of the experimental work each day to ensure consistency and stability of the system, so that the results could be accurate. The procedure for conditioning involves first putting the X-ray control unit on standby mode and then a programme code selected. The appropriate code is based on the last time the tube was conditioned. The following codes are available: 101, 102 and 103 corresponding to 1-3 days, 3-14 days and 2-6 weeks respectively. The key is then turned in the ON position and the irradiate/start button pressed on. The start time is recorded and the tube allowed to ‘‘warm up’’ to 280 kV before pressing stop button. The stopping time is then recorded. The difference between the stopping and the starting times gives the total time taken. After the conditioning, the environmental parameter which includes ambient temperature, atmospheric pressure and relative humidity are recorded before the start of the experiment. According to ISO-4037 which was first published in 1979, the range of values for ambient temperature, atmospheric pressure and relative humidity at standard test conditions are given as 291.15 K to 295.15 K, 86 kPa to 106 kPa, and 30 % to 75 % respectively. Working outside this range results in reduced accuracy. The reference values for temperature, atmospheric pressure and relative humidity during calibration are also given as 293.15 K, 101.3 kPa and 65 % respectively for the ionization chamber used. Corrections are therefore applied for changes in air pressure and temperature from the reference calibration conditions.

3.2.1.2 Beam Modification

The ionization chamber was pre-irradiated for five minutes to eliminate all unwanted charges within the chamber. The *HVL* determined for the N-60 to N-250

radiation qualities and the beam modified where necessary using added filtration to agree with ISO-4037 values. The experimental set-up is shown in Plate 3.6. The X-ray tube current was maintained at 10 mA. For each radiation quality the readings were made for 10 minutes at 1 minute interval. The mean reading obtained represents the exposure charges for a particular tube voltage and current. The *HVLs* were measured at a distance of 1 m from the focal spot. During the modification the thickness of Al or Cu that was used could not be predicted but experimentally obtained. Appendix 1 gives a summary of ISO4037 *HVL* for various X-ray beam qualities. The X-ray beam used in calibration must conform to these recommended standardized values.

The tube potential is measured under load according to the ISO-4037 standard, except for the five lowest energies, where the recommended inherent filtration is 1 mm Be, the total filtration consists of the additional filtration plus the inherent filtration adjusted to 4 mm aluminium. For these five lowest energies the recommended inherent filtration is 1 mm Be but other values may be used provided that the mean energy is within ±5% and the resolution within ±15% of the values given in the table (IAEA, 2000).

Once ISO4037 values were achieved the combination of material that gives the ISO values were transferred to the inherent filtration. The air kerma rates were then determined for the narrow series energies.

3.2.2 Air kerma Measurements from the X-ray Source

Using the experimental set-up shown in Plate 3.7 the air kerma rates were determined from 1m to 5m at 0.5m interval for x-ray qualities N-60, N-80, N-100, N-150, N-200 and N-250at tube current of 10mA.

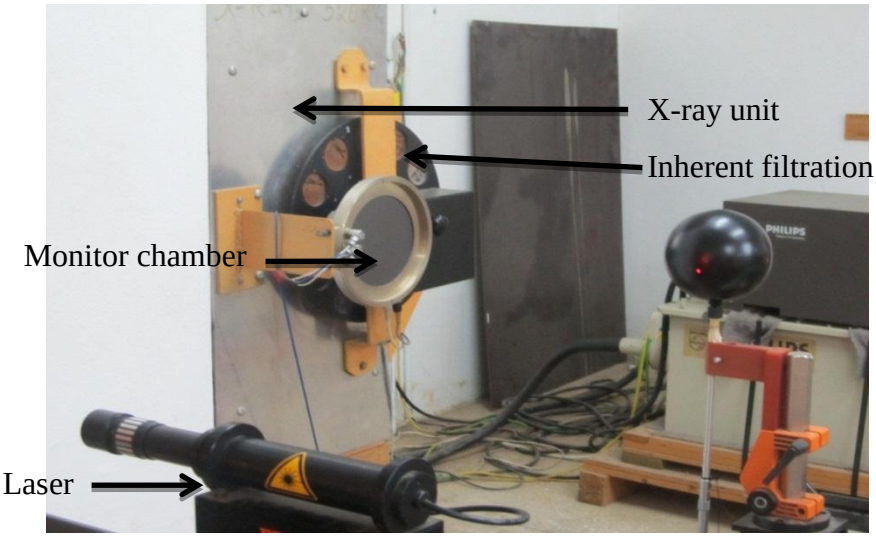

Plate 3.7: Experimental set-up for air kerma measurement in X-ray beam

The SSDL standard chamber was fixed on a holder mounted to the calibration bench, positioned at the reference distance and aligned to the X-ray beam. In the process, the laser alignment systems were used to check that the standard chamber is correctly positioned at the desired source–detector distance. The standard chamber was then connected to the electrometer and allowed30 minutes to establish equilibrium before irradiation. The high voltage was set to -250 V and the chamber is irradiated for at least 15 minutes before taking measurements. The irradiation time was set to 20 minutes and a series of 10 charge readings were taken using 60 seconds collecting time. The mean reading obtained at each distance was used to calculate the air kerma rates and ambient dose equivalent. Air density corrections to the readings are made based on measurements with the barometer and thermometer. No correction for humidity was made provided that it lies within the range 20% to 70% RH, over which the humidity correction is constant to within 0.1% (IAEA, 2000). The leakage current compared to the output was small so no significant impact on calibration factor, however there is the need to always do background reading for both dose profiling and calibration. This reading was subtracted from the exposure reading to

give the corrected exposure reading. The air kerma rates $\dot{K}_{ref}$ at the reference calibration points were determined using equation (3.3) (IAEA, 2000).

$$\dot{K}_{ref} = \frac{Q}{t} \times K_{PT} \times N_K \times K_Q \times K_{ot} \qquad (3.3)$$

where

$\dot{K}_{ref}$ was the air kerma rate in ($\mu Gy/s$),

Q the charges measured in (nC) and is given as the difference between the ionization chamber reading and the measured background,

t was the time taken to measure the charges in seconds,

N_K is the air kerma calibration factor of the chamber and electrometer in ($\mu Gy/nC$) (calibrated at IAEA). The calibration factors are shown in Appendix 3 for both ^{137}Cs γ-rays and X-ray qualities of 60 kV to 250 kV,

K_Q is a correction for the effect of any difference between the qualities of the beams at the IAEA and at the SSDL. This factor is unity since both are ^{137}Cs γ-rays and X-rays,

K_{ot} is correction factor to account for all other sources such as change in source position and contribution of scatter radiation. Their overall contribution is indeed negligible for this facility and

K_{PT} is the pressure and temperature correction factor which obeys the ideal gas law given by equation (3.4),

$$K_{PT} = \frac{101.325 \times (273.15 + T_m)}{293.15 \times P_m} \qquad (3.4)$$

The figures, 101.325 (in kPa) and 293.15 (in kelvin), are the reference pressure and temperature conditions, respectively, during the calibration of the chamber. T_m and P_m are the temperature and the pressure conditions, respectively, at the time of establishing the dose profile. T_m is the mean of the initial and final temperature reading in degrees Celsius and P_m is the mean of the initial and final pressure reading in kPa .

The results of the air kerma rate free-in-air measurements were used to calculate the required ambient dose equivalent, $H^*(10)$ at the calibration point using air kerma to ambient dose equivalent conversion coefficient (h) given in the ICRU Report 57 (ICRU,1998). Thus

$$H^*(10) = \dot{K}_{ref} \times h \qquad (3.5)$$

The values of h for x-ray are given in Table 2.2. $H^*(10)$ is the conventional true value or the reference value of the dose rate quantity to be measured.

The instrument used to measure the ambient dose equivalent had isotropic response.

3.2.3 Air kerma Measurements from the ^{137}Cs Source

Plate 3.8 shows the experimental set-up for the measurement of air kerma rates from 1m to 5m at 0.5m interval for the ^{137}Cs source.

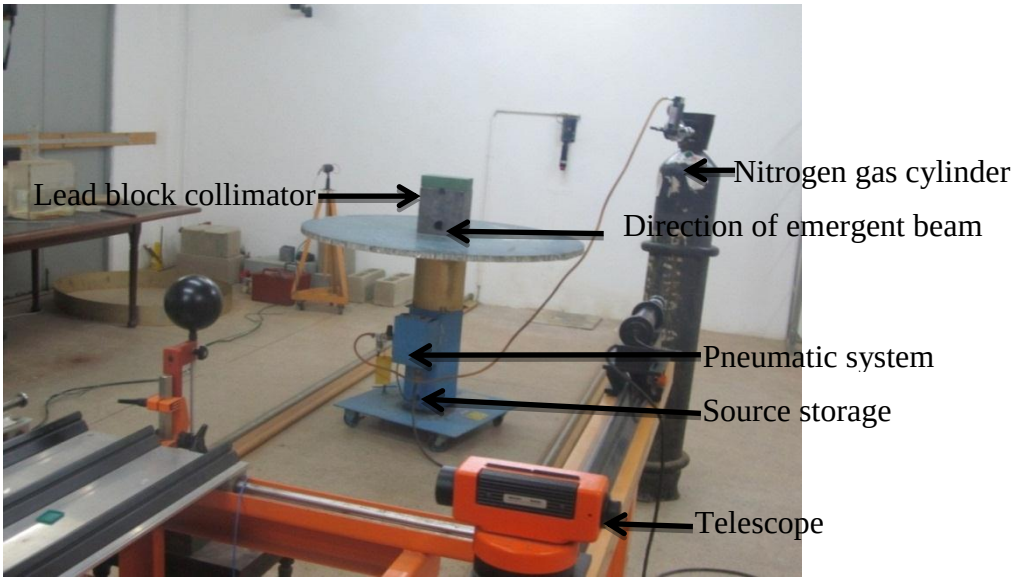

Plate 3.8: Experimental set-up for air kermameasurement in ^{137}Cs γ-rays

The SSDL reference standard ionization chamber was positioned at the reference distance and aligned to the ^{137}Cs gamma ray beam. The irradiation time is set to 40 minutes and a series of 10 charge readings were taken using 120 seconds collecting time. The mean reading obtained at each distance was used to calculate the air kerma rates and ambient dose equivalent. For every exposure, the laboratory parameters recorded were pressure, temperature and relative humidity (Knoll, 1999; Roberson et al, 1992; Piesch, 1981).The mean reading obtained at each distance was used to calculate the air kerma rates and ambient dose equivalent.

The air kerma rates at the reference distances were determined using equation (3.3) and converted to ambient dose equivalent using equation (3.5). The values of h for ^{137}Cs source are given in Table 2.3.

The ^{137}Cs undergoes radioactive decay and as time elapses, the initial activity relates to the activity as of the time of using the source by the expression.

$$A = A_o e^{-\lambda t} \qquad (3.6)$$

where

A is the present activity,

A_o is the initial activity at a known time,

λ is the decay constant and

t is the time to the date of exposure.

In other to correct for the decay of the ^{137}Cssource to the date of calibration, the following equation was used to determine the air kerma rate at that point of interest on that date.

$$\dot{K}_{ref,air} = \dot{K}_{ref}\, e^{-\frac{\ln 2}{t_{1/2}}t} \tag{3.7}$$

where

$\dot{K}_{ref,air}$ is the dose equivalent rate in $mSvh^{-1}$ after time, t, at the point of interest of the measurement,

$\dot{K}_{ref}$ is the initial dose equivalent rate at the time of measurement at the same point of interest at the reference time,

$t_{1/2}$ is the half-life of the ^{137}Cs source which is given as 30.17 years and

t is the days elapsed since the reference dose rate quantity was last determined.

3.2.4 Estimation of Calibration Factors

Dosimeter to be calibrated is placed with its reference point at the point of test, exposed to a nominal $H^*(10)$ and the indicated value is taken. The calibration factor (CF) of the instrument is estimated using Equation (3.8) (IAEA, 2000).

$$CF = \frac{H^*(10)}{\left(M_I - M_{B,I}\right) \times K_{PT,I}} \quad (3.8)$$

Where

M_I is the average survey meter readings normalised to standard conditions,

$M_{B,I}$ is the measured background by the survey meter,

$K_{PT,I}$ is the pressure and temperature correction factor for the calibration of the survey meter given by equation (3.4) and

$H^*(10)$ is the ambient dose equivalent at the time of calibrating the survey meter which is corrected for decay using Equation (3.9).

$$H^*(10) = h \times \dot{K}_{ref,air} \quad (3.9)$$

Combining equations (3.7) and (3.9) gives

$$H^*(10) = h \times \dot{K}_{ref}\, e^{-\frac{\ln 2}{t_{1/2}}t} \quad (3.10)$$

where, h is the ambient dose equivalent conversion coefficient for the ^{137}Cs source given in Table 2.3.

3.2.5 Theoretical Calculation of Reference Dose rates

The theoretical calculations of reference values are based on elapsed time. The reference dose equivalent rate on 18th July 2012 at the calibration distance of 1m was 2.046 mSvh^{-1}.Hence on the 22nd January 2013 (i.e. 188 days) the reference dose equivalent rate was determined using equation (3.10) which is expressed as

$$H^*(10) = h \times \dot{K}_{ref}\, e^{-\frac{\ln 2}{t_{1/2}} t}$$

where,

$h = 1.20$

$\dot{K}_{ref} = 2.046 mSv h^{-1}$

$t = 188$ days and

$t_{1/2}$ = 30.17 years.

The reference dose rate was then calculated at 1.5m, 2m, 2.5m, 3m, 3.5m, 4m, 4,5m and 5m based on the inverse square law given by equation (3.11) below.

$$D_a = \frac{D_1}{r^2} \qquad (3.11)$$

where

D_1 is the dose rate at 1m,

r is the distance from the source and

D_a is the dose rate at a particular distance from the source.

3.2.6 Uncertainty Components in Protection Level Calibrations

The uncertainty budget for the measurement of the calibration factors of the survey meters at the Ghana SSDL includes the uncertainty components of the mean reading of the survey meters using Equations 2.15 to 2.18, standard ionisation chamber calibration referred from the calibration certificate, pressure and temperature measurements and the positioning of the system. The uncertainty due to the pressure and temperature correction factor is given by the following equation:

$$\frac{U_{K_{PT}}}{K_{PT}} = \sqrt{\frac{U_P{}^2}{P^2} + \frac{T^2}{(273.15+T)^2} \times \frac{U_T{}^2}{T^2}} \qquad (3.12)$$

where

$U_{K_{PT}}$ is the uncertainty component of the pressure and temperature correction factor,

U_P is the uncertainty of the pressure component which includes the uncertainty from barometer calibration, uncertainty from mean reading and barometer resolution and

U_T is the uncertainty of the temperature component as a result of the uncertainty of mean reading of the temperature, thermometer calibration and the thermometer resolution.

Equation (3.12) was used to estimate the uncertainties due to air density for both the calibration of the reference ion chamber and the survey meter.

The uncertainty due to the ambient dose equivalent, $H^*(10)$ is given by the following equation:

$$\frac{U_{H^*(10)}}{H^*(10)} = \sqrt{\left(\frac{U_{(M_C - M_{B,C})}}{M_C - M_{B,C}}\right)^2 + \left(\frac{U_{K_{PT}}}{K_{PT}}\right)^2 + \left(\frac{U_{N_K}}{N_K}\right)^2 + \left(\frac{U_h}{h}\right)^2} \qquad (3.13)$$

Where

$U_{H^*(10)}$ is the uncertainty of the ambient dose equivalent,

$U_{(M_C - M_{B,C})}$ is the uncertainty component of the mean reading of the ionisation chamber in establishing the air kerma free-in-air,

U_{N_K} is the uncertainty component of the standard ionisation chamber calibration referred from the calibration certificate (Appendix 3) and

U_h is the uncertainty of the dose conversion coefficient which is recommended to be 2 % and this include calibration using the ^{137}Cs.

Therefore, the uncertainty due to the calibration factor (CF) of a given survey meter is given in the following equation:

$$U_{CF} = \frac{H^*(10)}{M_I - M_{B,I}} \times \sqrt{\left(\frac{U_{H^*(10)}}{H^*(10)}\right)^2 + \left(\frac{U_{(M_I - M_{B,I})}}{M_I - M_{B,I}}\right)^2 + \left(\frac{U_{K_{PT}}}{K_{PT}}\right)^2} \qquad (3.14)$$

where

U_{CF} is the uncertainty due to the calibration of the survey meter and

$U_{(M_I - M_{B,I})}$ the uncertainty component of the survey meter readings.

In terms of the abovementioned uncertainty components, the combined standard uncertainty is then given by:

$$U_C = \sqrt{u_A^{\,2} + u_B^{\,2} + u_C^{\,2} + u_D^{\,2} + u_E^{\,2} + u_F^{\,2} + u_G^{\,2}} \qquad (3.15)$$

The overall uncertainty in the calibration of a survey meter is expressed as an expanded uncertainty at 95 % confidence level (k=2) (Lewis et al, 2003).

3.2.7 Irradiation of Thermoluminescent Dosimeters (TLDs)

To ensure the reliability of the experimental results, the process must be validated. This was done by placing four TLD cards containing lithium fluoride chip (LiF) on the standardized designed ICRU slab phantom to cater for backscatter conditions of the human body as shown in Figure 3.1.

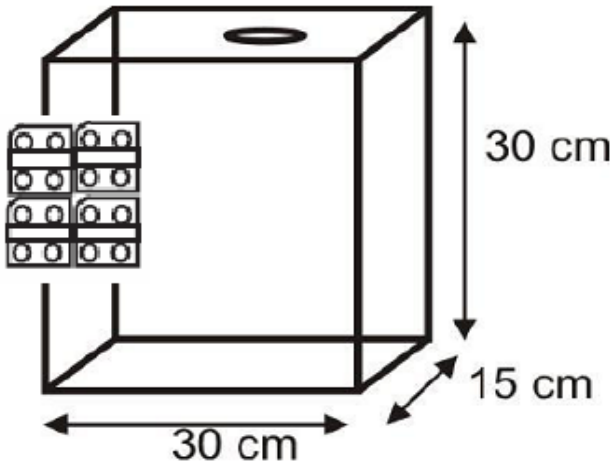

Figure 3.1: TLD fastened to ICRU slab phantom

The TLDs were then exposed to ^{137}Cs gamma-rays whilst the set-up at the laboratory was still maintained. The exposure was done at the reference distance of 1m and for doses of 1 mSv, 2 mSv and 3 mSv. The TLDs were then read at the Personnel Monitoring Service Laboratory using HARSHAW 6600 TLD reader and their results compared to those obtained using the SSDL standard ionization chamber (Horowitz, 1990).

The time needed to deliver these doses was calculated based on the established dose profile in this work.

TLDs are used in SSDL and personnel monitoring services because their dose responses cover a wide range of dosimetric values, have linear dose response characteristics and are able to score the correct physical doses. They have a wide dosimetric range; meaning they can measure very low and very high doses, therefore have a wide useable range (Annkah et al, 2011).

CHAPTER FOUR

RESULTS AND DISCUSSION

This chapter presents the results that were obtained from the experiments which are adequately discussed.

4.1 Results of *HVL* Determination

The *HVL* was first determined to ensure that the energies of the X-ray photons were correct before establishing the dose profiles. The results obtained during measurement of charges for 60 kV is given in Table 4.1.

Table 4.1: Measurement of charges for 60 kV 10mA,60 seconds

Thickness of Cu (mm)	Charges(nC)				
	Q 1	Q 2	Q 3	Q 4	Q Average
0.00	13.650	13.590	13.600	13.590	13.608
1.00	0.927	0.914	0.931	0.926	0.925
1.41	0.371	0.370	0.389	0.374	0.376

Using the charges measured in Table 4.1 attenuation curve was generated for the 60 kV radiation by plotting the graph of Cu thickness versus the average charges measured per minute as shown in Figure 4.1 below.

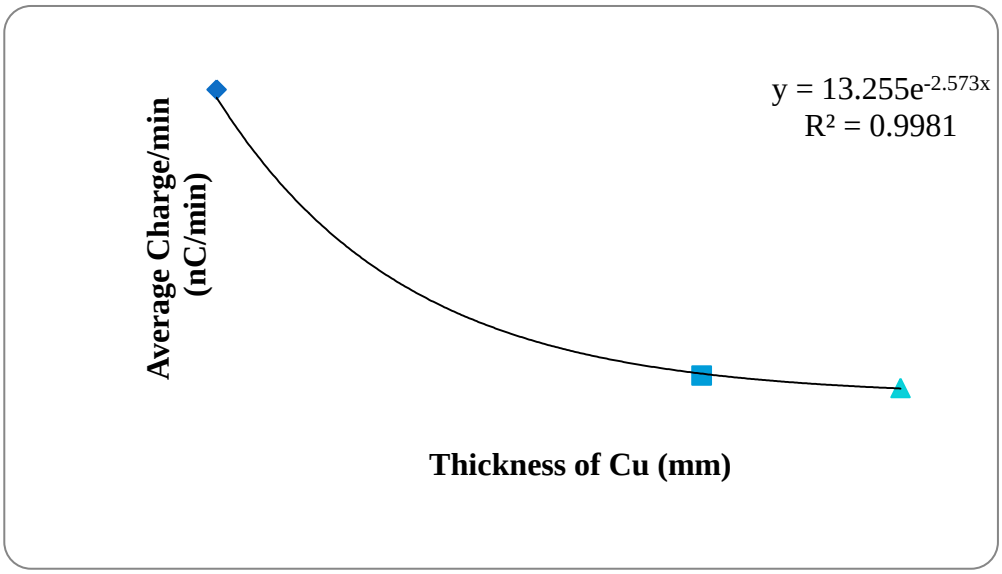

Figure 4.1: Attenuation curve generated for 60 kV

From this graph the line of best fit is generated which is given by equation 4.1 as:

$$y = 13.255\, e^{-2.573x} \qquad (4.1)$$

When equation 4.1 is compared to the general radiation transmission and shielding equation given in equation 3.1, it can be observed that the linear attenuation coefficient (μ) is equal to 2.573 mm^{-1} yielding an average *HVL* value of 0.27 mm Cu. The *HVL* obtained exceeds the ISO and SSDL reference standard ionization chamber value which is 0.24 mm Cu. The percentage deviations of the calculated (measured) *HVL* from the ISO and SSDL reference ionization chamber values are respectively 10.5% and 9.5%, which is above the limit of 2%. Hence, the need to modify the beam with a new set of added filtration.

It is also observed from the graph that the experimental results and the line of best fit drawn for the set of data is in agreement showing an R^2 value of 0.9981.

The thickness of Al and Cu used for the study was modified experimentally by using 0.7 mm Al. The attenuation curve generated for the 60 kV radiation (modified) beam is given in Figure 4.2.

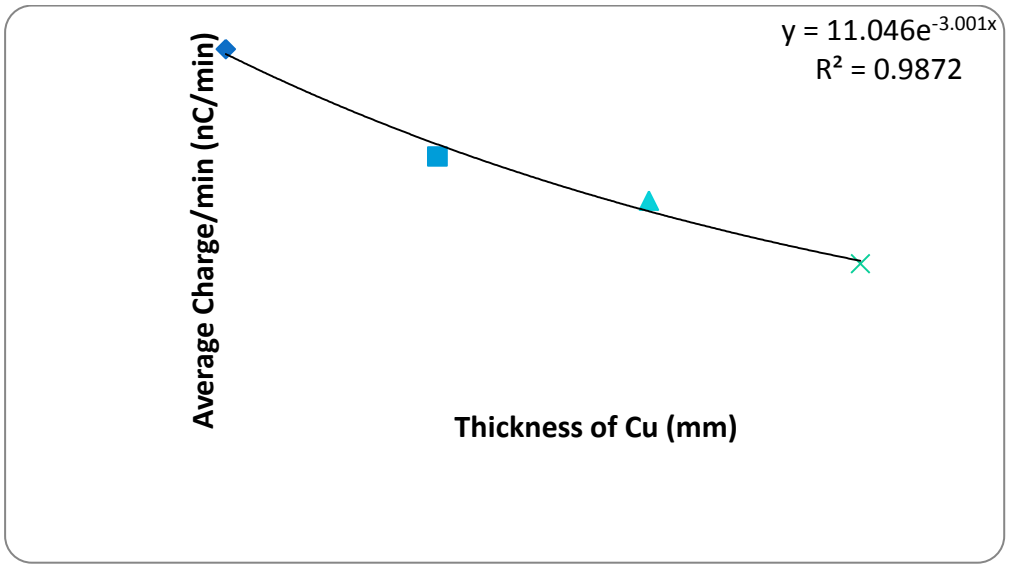

Figure 4.2: Attenuation curve generated for 60 kV(modified)

From this graph is observed again that the line of best fit is generated given by equation 4.2 as:

$$y = 11.046\, e^{-3.001x} \qquad (4.2)$$

Equation 4.2 was compared to the general radiation transmission and shielding equation (equation 3.1), it can be observed that μ = 3.001 mm^{-1}yielding an average *HVL* of 0.23 mm Cu. The *HVL* obtained was in close agreement with the SSDL reference chamber and the ISO value of 0.24 mm Cu at 60 kV with a deviation of less than 2% and was therefore considered acceptable (IAEA, 2009).

It was observed from Figure 4.2 that the correlation between the points had a value of 0.9872. Hence for 60 kV an added filtration of 0.7 mm Al was required to modify the beam to obtain a value which was in agreement with the ISO value of 0.24 mm Cu at 60 kV.

The gradients (linear attenuation coefficients, μ) of the curves generated for the determination of *HVL* reduce as the values of kV increase indicating an inverse relationship. Physically, this means that for a given unit thickness of an absorber material, its effectiveness for removing the photons from the X-ray beam is reduced as X-ray tube potential increases.

By plotting the graph of Cu thickness versus average charges measured per minute given in Tables 4.2 to 4.6, attenuation curves were also generated for 80 kV, 100 kV, 150 kV, 200 kV and 250 kV These are presented in Appendix 1 and were used to determine the *HVL*.

Table 4.2: Measurement of charges for 80 kV 10 mA, 60 seconds

Thickness of Cu(mm)	Charges(nC)				
	Q 1	Q 2	Q 3	Q 4	Q Average
0.00	6.202	6.211	6.194	6.175	6.200
1.00	1.897	1.928	1.917	1.928	1.920
1.41	1.246	1.240	1.227	1.226	1.230

Table 4.3: Measurement of charges for 100 kV 10 mA, 60 seconds

Thickness of Cu(mm)	Charges(nC)				
	Q 1	Q 2	Q 3	Q 4	Q Average
0.00	2.801	2.819	2.801	2.815	2.810
1.00	1.510	1.508	1.514	1.512	1.510
1.41	1.211	1.176	1.208	1.186	1.200

Table 4.4: Measurement of charges for 150 kV 10 mA, 60 seconds

Thickness of Cu(mm)	Charges(nC)				
	Q 1	Q 2	Q 3	Q 4	Q Average
0.00	21.410	21.380	21.410	21.430	21.410
1.00	15.980	16.080	15.910	15.960	15.980
1.41	14.160	14.220	14.210	14.250	14.210

Table 4.5: Measurement of charges for 200 kV 10 mA, 60 seconds

Thickness of Cu(mm)	Charges(nC)				
	Q 1	Q 2	Q 3	Q 4	Q Average
0.00	7.390	7.459	7.356	7.424	7.410
1.00	6.299	6.259	6.226	6.267	6.260
1.41	5.803	5.845	5.829	5.801	5.820

Table 4.6: Measurement of charges for 250 kV 10 mA, 60 seconds

Thickness of Cu(mm)	Charges(nC)				
	Q 1	Q 2	Q 3	Q 4	Q Average
0.00	8.814	8.851	8.825	8.804	8.820
1.00	7.764	7.784	7.631	7.712	7.720
1.41	7.323	7.346	7.386	7.328	7.350

The *HVLs* determined for these energies were found to agree closely with the ISO values. Measurements of these qualities were made as a function of time. The measured *HVL* compared with the ISO and SSDL reference ionisation chamber *HVL* values are presented in Table 4.7.

Table 4.7: ISO and SSDL chamber *HVL* compared with measured *HVL*

Radiation Quality (kV)	ISO HVL (mm Cu)	SSDL chamber HVL (From calibration certificate) (mmCu)	Measured HVL (mmCu)	Measured HVL (mmCu) Modified
60	0.24	0.24	0.27	0.23
80	0.58	0.59	0.60	
100	1.11	1.15	1.13	
150	2.36	2.40	2.38	
200	3.99	4.06	4.08	
250	5.19	5.21	5.28	

Table 4.7 shows that as the kV increases, so does the average energy of the x-ray photons in keV. This increase in energies are responsible for the increasing *HVL* figures, since thicker materials are needed to reduce the intensity of the X-ray beams as photon energies increase (Jozela, 2007). The higher the energy of a photon, the more interaction with the absorber is needed in order to remove it from the beam, hence the need for a thicker absorber material which will ensure more collisions (scattering) within the absorber material and hence loss of energy of the photon and eventual removal from the X-ray beam.

The errors in the specification of kilovoltage beam quality can be attributed to the experimental setup of the measurement of *HVL*. Errors are also introduced from lack of stability in beam output. International Codes of practice advise users to introduce a monitor chamber to monitor the variation in machine output during such a suite of measurements. The effectiveness of using a monitor chamber in the determination of *HVL* has been shown to be significant in this work. These measurements also require high purity filters.

Also there appears to be a linear relationship between the kV potential that the X-ray tube is subjected to and the *HVL*.Comparison of the measured *HVL* values with

ISO 4037 *HVL*, SSDL chamber *HVL* and the modified *HVL* is illustrated graphically in Figure 4.3.

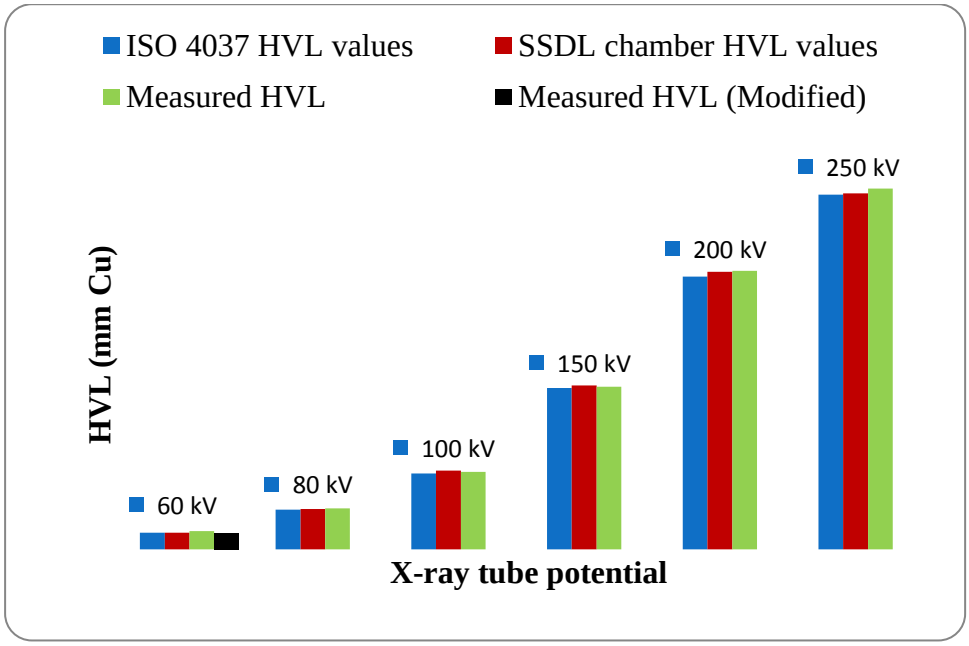

Figure 4.3: Comparison of *HVL* values

The *HVL* obtained is consistent with the ISO values, which indicates that the equipment is calibrated at IAEA. The slight variations may be attributed to the age of the machine since it has been installed for a long time and due to prolong use. Hence there is a slight reduction in the efficiency of the machine.

Another contribution to the deviation is the electrometer and the connecting cable. Also the wear and tear of filter thickness, may contribute to the deviation. Uncertainty in the measurement of the thickness of the filters may also contribute to the deviations.

For 80 the kV to 250 the kV no modification was done on the emitted beam since the measured HVL values were in close agreement with the ISO and SSDL chamber HVL values.

The percentage deviations of the measured *HVL* from ISO and SSDL ion chamber *HVL* values are presented in Table 4.8.

Table 4.8: Percentage deviations from ISO and SSDL chamber values

Radiation Quality (kV)	% Deviation of measured HVL from ISO values	% Deviation of measured HVL from SSDL chamber values
60	10.50	9.50
80	3.07	1.30
100	2.01	1.56
150	0.72	0.97
200	2.19	0.43
250	1.77	1.36

The table compares the *HVLs* obtained in this work to those stated as the 1st *HVL* values by IAEA Safety Reports Series No.16 as well as those quoted on the calibration certificate of the SSDL reference ionization chamber. The figures from the IAEA Safety Reports Series No.16 are recommended and provide a general context and background from which *HVL* figures from tests on x-ray machines can be interpreted. On the other hand, the figures on the calibration certificate are specific to the reference instrument used in the experiment thus it(calibration certificate figures) is the main criteria for determining suitability of beam or not. For the 1st *HVL* values, the percentage deviation is less than 4% except for 60 kV which is approximately 10%. However, the % deviations with the values quoted on the calibration certificate of the SSDL reference ionization chamber, for the various kVs are less than 2% except for the 60kV. The 2% threshold of variation is acceptable, however higher values are not, thus the 60 kV was modified experimentally by using 0.7 mm Al. These results indicate that for all the kVs except for 60kV, the X-ray machine is emitting X-rays of the prescribed energies. And thus all other experiments can proceed. This is illustrated graphically in Figure 4.4.

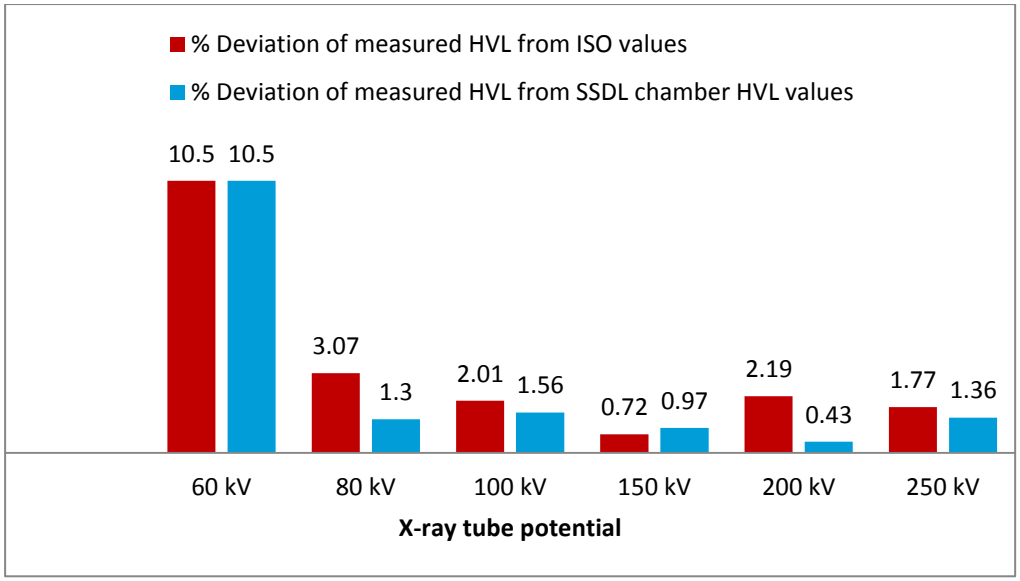

Figure 4.4: Percentage deviations from ISO and SSDL chamber *HVL*

In this work, attenuation curves have been generated for 60kV to 250 kV as shown in figures 4.1 and 4.2 and figures in Appendix 1 which were used to determine the *HVL*..

4.2 Ambient Dose Measurements in Narrow Beam X-ray

The results of air kerma free-in-air measurements were used to calculate the required ambient dose equivalent, $H^*(10)$ at the calibration points using the air kerma to ambient dose equivalent conversion coefficients given in the International Commission on Radiation Units and Measurements (ICRU) Report 57.

The results obtained during measurement of charges for X-ray tube potentials of 60 kV to 250 kV at the reference distances of 1m to5m is presented in Appendix 2. Table 4.9 below gives the summary of the charges obtained from which the air kerma was determined.

Table 4.9: Correct exposure reading from X-ray unit

Reference Distance (m)	Charges (nC)					
	60 kV,10 mA	80 kV,10 mA	100 kV,10 mA	150 kV,10 mA	200 kV,10 mA	250 kV,10 mA
1.0	11.015	7.870	3.447	28.800	9.854	7.835
1.5	4.931	3.682	1.961	12.680	4.305	4.018
2.0	3.045	2.091	1.804	8.156	3.361	2.115
2.5	2.052	1.993	1.370	5.079	2.082	1.899
3.0	1.950	1.494	0.999	4.055	1.612	1.393
3.5	1.451	1.369	0.764	3.213	1.272	1.191
4.0	1.269	1.047	0.614	1.973	0.937	0.566
4.5	1.034	0.720	0.560	1.719	0.783	0.292
5.0	0.917	0.612	0.437	1.059	0.563	0.208

From Table 4.9, it is observed that as the distance from the focal point of the X-ray machine increases, the amount of charges recorded per unit time of 1 minute reduces. This is in conformity with the inverse square law that governs radiations.

Using the charges measured from Table 4.9 and the calibration coefficient for the SSDL reference standard chamber given in Appendix 3, the air kerma rates $\dot{K}_{air}$ were calculated using equation (3.3) and converted to ambient dose equivalent $H^*(10)$ using equation (3.5).

4.2.1 SSDL Chamber at Reference Distance of 1 m

During the exposures at this distance, laboratory parameters were recorded at initial pressure P_i of $100.8\,kPa$, final pressure P_f of $100.6\,kPa$, initial temperature T_i of $25\,^oC$,final temperature T_f of $23.1\,^oC$, initial and final Relative Humidity (R.H) of 55%.Using equation (3.4) the pressure and temperature correction factor K_{PT} was 1.02.

For N-60 modified x-ray quality

Charge $Q = 11.015\,nC$ (4.3)

Time $t = 60\,\text{sec}$,

Calibration coefficient $N_K = 25.3\,uGy/nC$

Substituting the above values in equation (3.3) gives

$$\dot{K}_{air} = \frac{11.015}{60}\left(\frac{nC}{s}\right) \times 1.02 \times 25.3\left(\frac{\mu Gy}{nC}\right) \quad (4.4)$$

$\dot{K}_{air} = 4.7376\ \mu Gy/s$

From equation (3.5)

$H^*(10) = \dot{K}_{air} \times h$

But for N-60 x-ray quality, $h = 1.59\ Sv/Gy$.

Hence

$$H^*(10) = 4.7376 \left(\frac{\mu Gy}{s}\right) \times 1.59 \left(\frac{\mu Sv}{\mu Gy}\right) \times 3600 \left(\frac{s}{h}\right) \qquad (4.5)$$

$H^*(10) = 27{,}118.02\ \mu Sv/h$

$H^*(10) = 27.118\ mSv/h$

The computation was repeated for all the X-ray qualities of 80 kV, 100 kV, 150 kV, 200kV and 250 kV. The calculation procedure is the same described above for the 60 kV. The dose profile generated in terms of air kerma rates ($\dot{K}_{air}$) is presented in Table 4.10.

Table 4.10: Dose profile generated for X-ray beam

Reference distance (m)	$\dot{K}_{air}$ (µGy/s)					
	60kV	80 kV	100 kV	150 kV	200 kV	250 kV
1.0	4.738	3.358	1.459	12.140	4.121	3.317
1.5	2.116	1.568	0.829	5.337	1.797	1.697
2.0	1.307	0.890	0.762	3.430	1.402	0.893
2.5	0.881	0.849	0.579	2.137	0.869	0.802
3.0	0.840	0.639	0.424	1.713	0.676	0.591
3.5	0.624	0.583	0.323	1.353	0.531	0.504
4.0	0.545	0.446	0.260	0.831	0.392	0.239
4.5	0.446	0.308	0.238	0.727	0.329	0.124
5.0	0.395	0.261	0.185	0.448	0.236	0.088

These doses will now serve as reference values that will be used as standards for calibration in the SSDL at the given time and under the set conditions. Figures 4.5 shows the dose profile curve established for the60 kV (modified) X-ray quality in terms of $H^*(10)$.

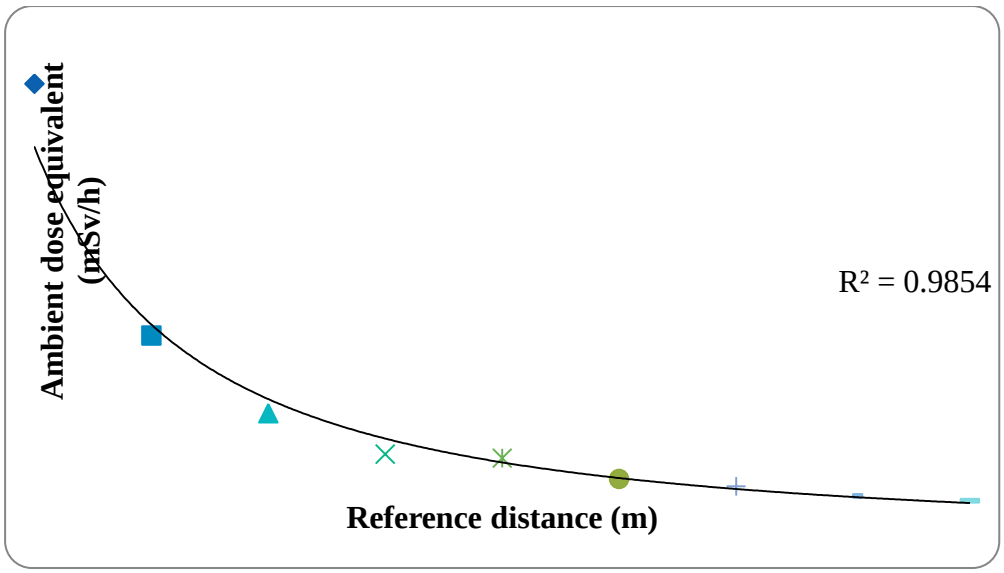

Figure 4.5: Dose profile curve established for 60 kV (modified)

This is in agreement with inverse square law given by equation (3.11). These imply that the detector's readings are accurate.

The dose profile curves established for 80 kV to 250 kV X-ray quality in terms of $H^*(10)$ follows the same trend and is presented in Figures 4.6 to 4.10.

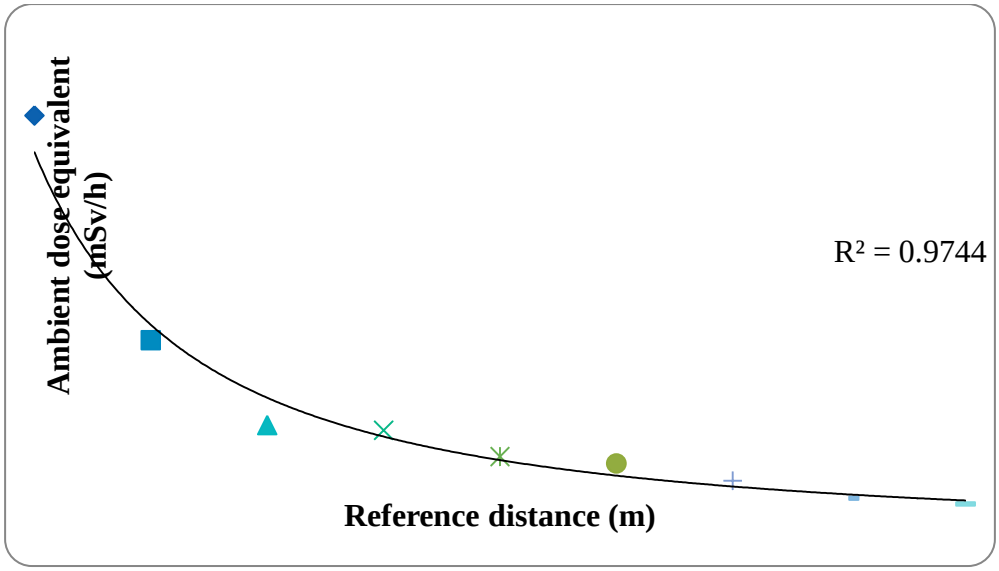

Figure 4.6: Dose profile curve established for 80 kV

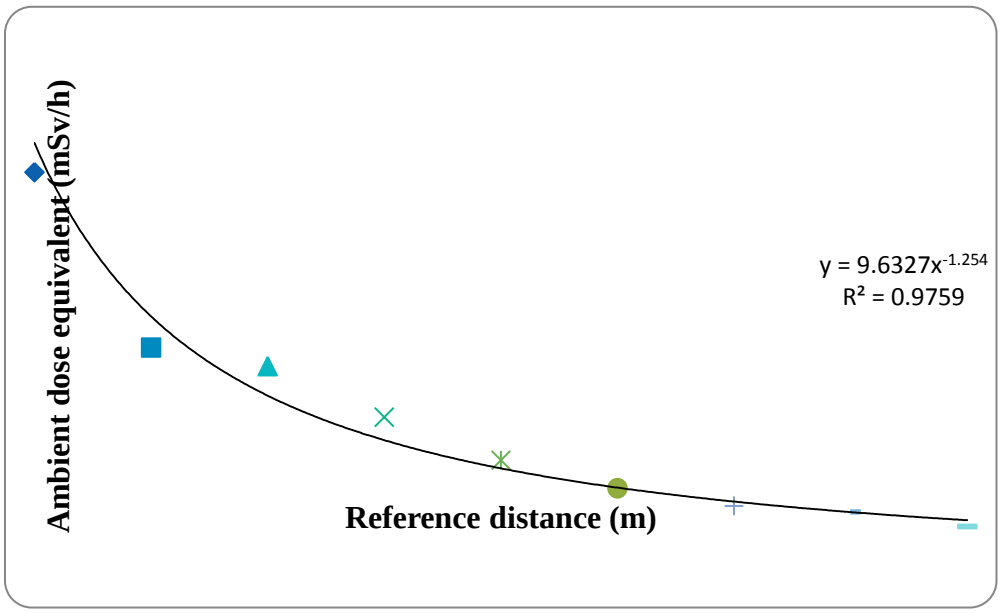

Figure 4.7: Dose profile curve established for 100 kV

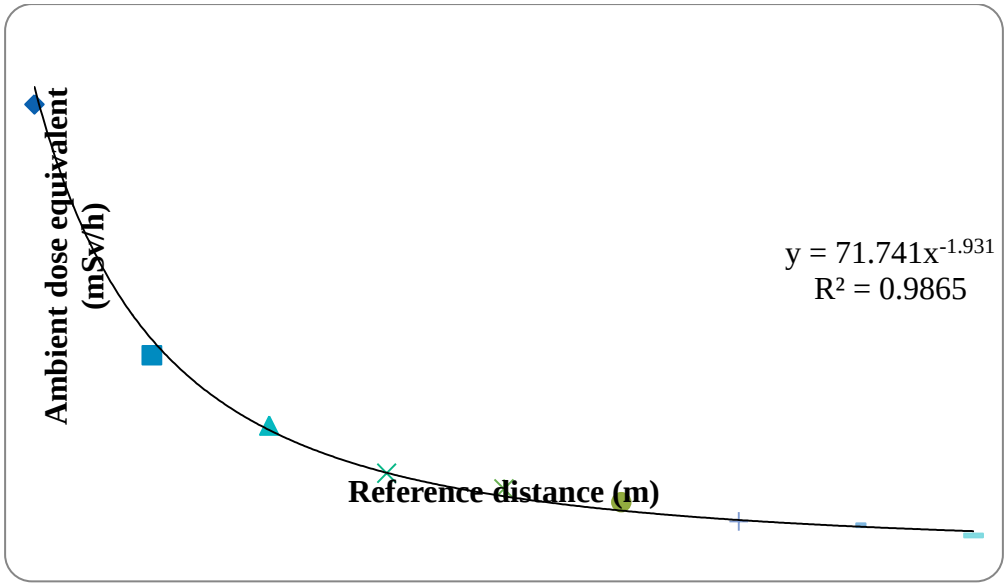

Figure 4.8: Dose profile curve established for 150 kV

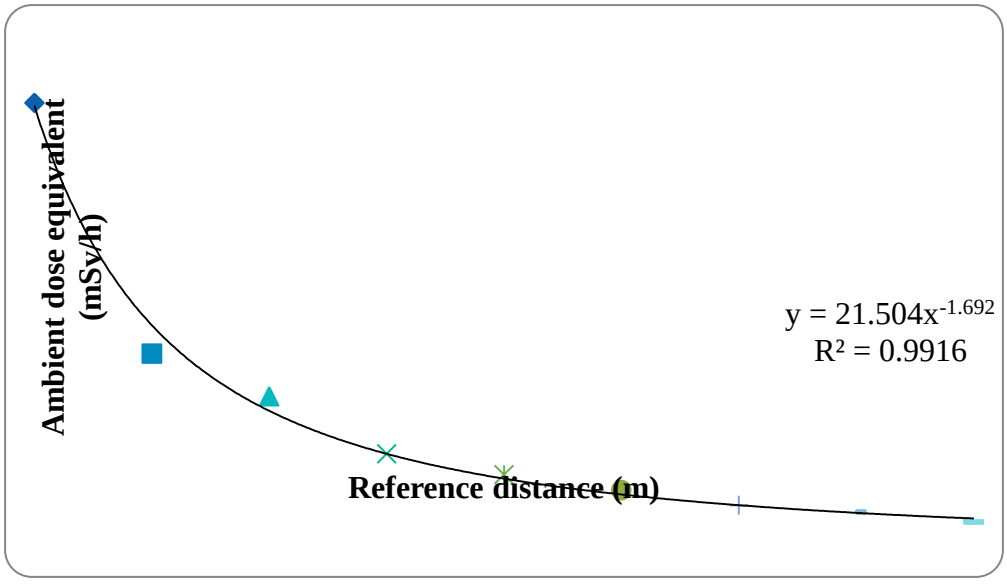

Figure 4.9: Dose profile curve established for 200 kV

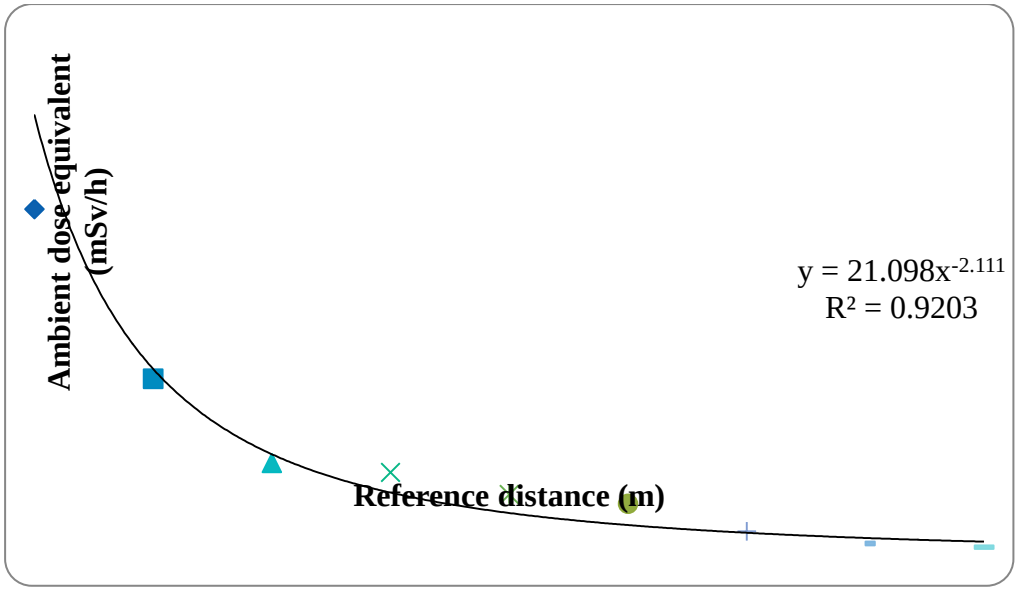

Figure 4.10: Dose profile curve established for 250 kV

4.3 Ambient Dose Measurements in ^{137}Cs Gamma Ray Beam

Tables 4.11 gives a summary of the results obtained during measurement of the charges at the reference distance of 1m to 5m from the ^{137}Cs source.

Table 4.11: Correct exposure reading from ^{137}Cs gamma irradiator

Reference Distance (m)	Correct Exposure Reading (nC)
1.0	2.039
1.5	0.823
2.0	0.685
2.5	0.481
3.0	0.448
3.5	0.445
4.0	0.369
4.5	0.275
5.0	0.221

Using Tables 4.11 and the calibration coefficient for the photon beams given in Appendix 3, the air kerma rates $(\dot{K}_{\text{air}})$ were calculated using equation (3.3) and converted to $H^*(10)$ using equation (3.5). The calculation procedure is the same as described above for the X-ray. During the exposures at this distance, laboratory parameters were recorded at initial pressure (P_i) of 100.8 kPa, final pressure (P_f) of 100.5 kPa, initial temperature (T_i) of 24 ºC, final temperature (T_f)of 23.1 ºC, and Relative Humidity (R.H) of 54%. Using equation (3.4) the pressure and temperature correction factor (K_{PT}) was of 1.02 value. The dose profile generated in terms of air kerma rates $(\dot{K}_{\text{air}})$ is presented in Table 4.12.

Table 4.12: Dose profile generated for the ^{137}Cs source

Reference Distance (m)	$\dot{K}_{air}$(µGy/s)
1.0	0.443
1.5	0.179
2.0	0.149
2.5	0.104
3.0	0.097
3.5	0.097
4.0	0.080
4.5	0.060
5.0	0.048

These doses will now serve as reference values that will be used for calibration in the SSDL at the given time and under the set conditions. Figures 4.11 shows the dose profile curve established for the collimated ^{137}Cs source in terms of $H^*(10)$.

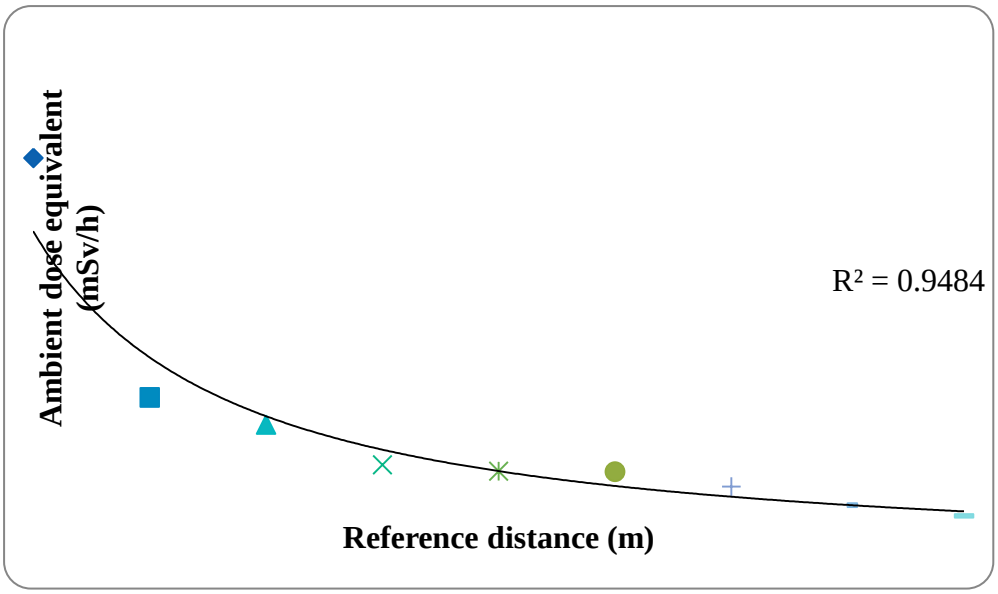

Figure 4.11: Dose profile curve established for ^{137}Cs source

This is typical of decay of radionuclides and also in agreement with inverse square law given by equation (3.11). These imply that the detector's readings are accurate and hence suitable for it intended purpose. It can be extrapolated from the dose rate measured at 1m to give the dose rates at 1.5m, 2m, 2.5m, 3m, 3.5m, 4m, 4.5m and 5m. Table 4.13 gives the theoretical dose rates values compared with the experimental values.

Table 4.13: Theoretical $H^*(10)$ values compared to measured values

Reference Distance (m)	Theoretical $H^*(10)$ (mSv/h)	Measured $H^*(10)$ (mSv/h)	% Standard deviation of measured dose rates
1.0	2.022	1.915	3.95
1.5	0.898	0.772	11.46
2.0	0.555	0.643	9.66
2.5	0.324	0.451	36.08
3.0	0.225	0.420	32.88
3.5	0.165	0.418	23.92
4.0	0.126	0.346	44.88
4.5	0.100	0.258	14.62
5.0	0.081	0.207	43.08

It can be noted that the standard deviation of the measured dose rate is about 4% at 1m whiles it is about 43% at 5m. It is evident that the further the distance is from the source centre the less consistent, and reliable the readings. This wide variation may be due to the scattering of radiation in air before reaching the detector or the broadening of the radiation beam. Other contribution to the variation includes random experimental errors, lower gas pressure influencing the source position and the fact that radiation emission is statistical. From 1m to 2m represents the best distances of measuring the dose rates since the standard deviation is generally less than 10%.

4.4 Uncertainty Analysis

Uncertainty contributors were identified during measurement of ambient dose equivalent $H^*(10)$. Table 4.14 gives the summary of the uncertainty analysis performed.

Table 4.14: Estimated standard uncertainty for ambient dose measurement

Physical quantity	Relative standard uncertainty (%)
Uncertainty in the calibration of the standard dosimeter, u_A	0.2
Establishment of the reference conditions, u_B	0.05
Repeatability of the measurements, u_C	0.18
Uncertainty of the dose conversion coefficient, u_D	0.02
Uncertainty in the temperature and pressure correction factors, u_E	0.02
Uncertainty in the measurement of the distance, u_F	0.1
Uncertainty in the dimensions of the slit, u_G	0.1
Combined standard uncertainty U_C	0.31

The survey meters for dose rate measurements within the industrial, medical and research facilities in Ghana are calibrated periodically and the results show that duringthe period 2008–2011, approximately 91% were within±20.0 %. The results for

this period indicate that most of the survey meters brought for calibration were within the regulatory requirement (Adjei et al, 2013).

Figure 4.12 shows the range of uncertainties in the estimation of the calibration factors of the set of survey meters calibrated at the SSDL in Ghana from 2008 to 2011.

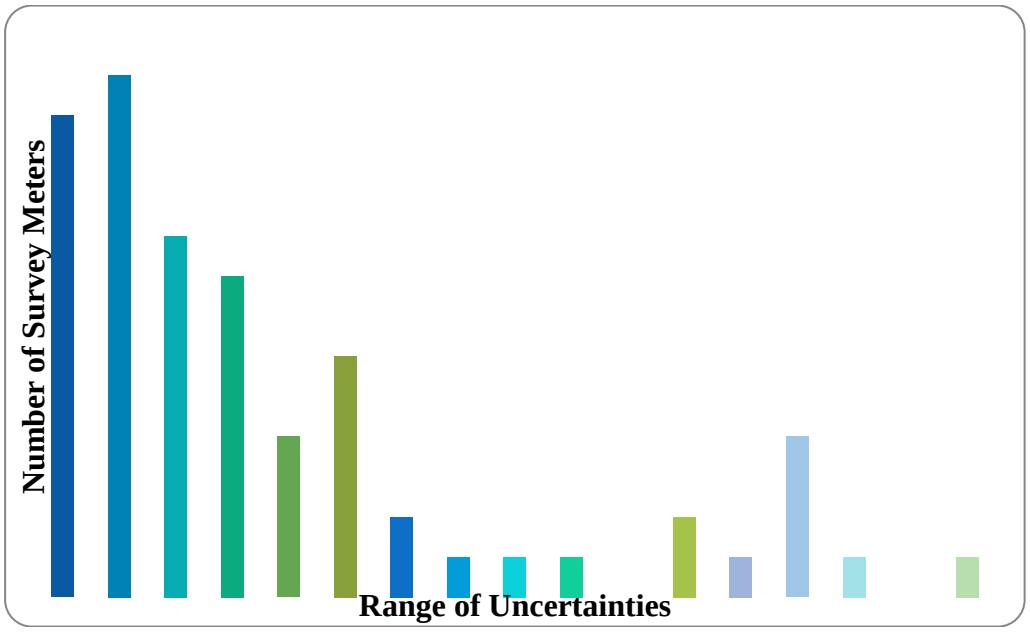

Figure 4.12: Range of uncertainties in estimation of calibration factors

The uncertainty ranged from 0.03 to 17 % with the majority of them ranging from 0.03 to 6.0 % with a few of them more than6.0 %. This indicates that most of the calibration factors with the associated uncertainties are within the acceptable limits (Adjei et al, 2013). From the calibration factors with the associated uncertainties obtained, it is obvious that the reference instrument is very accurate, has high sensitivity and very good radiation response. This is further confirmed by the dose profile generated using the equipment.

4.5 Response of TLD Cards to Irradiation

The TLD cards showed a linear dose response to the exposures of 1mSv, 2mSv and 3mSv in the gamma- rays at 1cm deep which is referred to as the $H_p(10)$ or deep dose as shown in Figure 4.13.

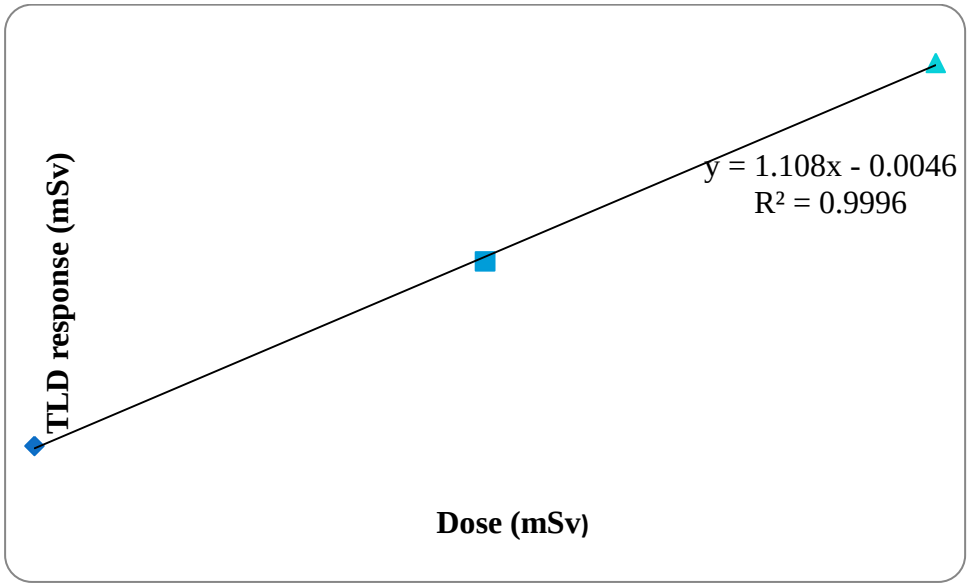

Figure 4.13: Response of TLD cards to irradiation

The R^2 value which is approximately equal to 1 indicates a good agreement, hence a validation of the experimental procedure, accuracy of equipment and reliability of the results. Table 4.15shows the data generated from irradiating the TLD cards.

Table 4.15: Result of irradiation of TLD cards

Exposure	Dosimeter ID	Reader's value (mSv)	%Deviation
1mSv @	600139	1.1268	12.68
1 m	600284	1.1013	10.13
	600471	1.1218	12.18
2mSv@	1301	2.1834	9.17
1 m	1302	2.2084	10.42
	1303	2.1628	8.14
3mSv@	600035	3.3528	11.76
1 m	600276	3.3171	10.57
	600523	3.3279	10.93

The 1mSv exposure yielded +10.13% as the minimum and +12.68% being the maximum deviation. The 2 mSv exposure yielded +8.14% as minimum while +10.42% being the maximum, 3 mSv exposure yielded +10.57% being the minimum and +11.79% as the maximum deviation. This showed that the response of the TLDs were within ±20%, therefore acceptable for regulatory purposes.

CHAPTER FIVE

CONCLUSIONS AND RECOMMENDATIONS

This chapter presents the conclusions and recommendations based on the study results.

5.1 Conclusions

Studies have been carried out to establish dose profiles for narrow beam X-rays and ^{137}Cs source at the SSDL of the Ghana Atomic Energy Commission. The X-rays gave an ambient dose equivalent of 0.44 mSv/h as the minimum and 69.1 mSv/h as the maximum and the ^{137}Cs source gave 0.21 mSv/h as the minimum and 1.92 mSv/h as the maximum.

The results from the study also indicated that the X-ray machine is emitting X-rays of the prescribed energies except for 60 kV which was subsequently modified by using 0.7 mm Al and its output measured at given distances were constant. Equipment with very low useable range (with respect to photon energy) can now be calibrated using the X-ray beam.

The results could serve as reference for calibration of all types of dosimetric instruments at the SSDL. This will enhance participation in intercomparison exercises, improve calibration services performed by the SSDL and minimise errors accompanied by radiation exposure during calibration. The data could also be used in the irradiation of samples and to compare subsequent work.

The study also highlighted the importance of dose standardization to ensure that radiation measurements are linked to the international system. The rapid growth

in the application of nuclear technology is obviously to be welcomed provided that radiation protection measures are being enhanced to ensure that the safety aspects really meet the required international standards.

The uncertainties associated with majority of the calibration factors for the set of survey meters calibrated at the SSDL in GAEC from 2008 to 2011 are within the acceptable limits. The uncertainty ranged from 0.03 to 17 % with the majority of them ranging from 0.03 to 6.0 % with only a few of them more than 6.0 %.

5.2 Recommendations

The HVL is one of the parameters to be checked regularly in a quality assurance programme. Its value is an index of the spectral quality of the x-ray beam and its experimental measurement requires narrow beam geometry. Therefore the following recommendations are addressed to various stakeholder institutions to improve calibration of radiation protection instruments:

5.2.1 Research Institutions and Service Organisations

Research institutions and organisations that provide calibration services to end users of equipment used for ionizing radiation measurements need to improve dosimetric accuracy and thereby ensure reliability of ionizing radiation measurements. They should promote the compatibility of dosimetric methods in order to achieve harmonization and uniformity of dosimetry in all ionizing radiation laboratories.

The radiation quality should be checked for stability at least annually. The results of stability test using radioactive check source measurements performed for

the reference standard ionization chamber must show a deviation less than 1.0% which is acceptable according to ISO 4037.

Whenever any part that could affect the beam quality is repaired or replaced, ISO 4037 requirements for beam quality should be met.

In order to reduce the degradation of the filter thickness it should be properly stored and handled. This will also ensure that the filter surfaces are not contaminated and their thickness is not eroded through wear and tear.

Filters should be made from metal with the highest purity readily available. They should be as homogeneous as possible, without visible flaws (pinholes, cracks, macroscopic grains). For materials which are not produced from standard laboratories purity test must be done before being used as filters to determine HVLs.

Quality control checks and recalibration must be done at regular intervals. The reference standard chamber should be calibrated at the Austrian National Primary Standards Laboratory in Vienna at least every five years and the results compared with previous calibration factor. This ensures that the calibration services provided by the laboratory follow internationally accepted metrological standards.

External dose quality audit must be maintained through participation in the IAEA annual intercomparison programme using ionization chambers and TLDs and deviation more than7.0% should be investigated and corrected on time. This ensures that the results obtained with the set up in the laboratory can be validated by other laboratories.

The laboratory is to advice, inform and guide the users of ionizing radiation on dosimetry issues as well as to exchange the experience and knowledge between users.

5.2.2 Regulatory Authority

The Regulatory Authority must ensure that recommended dose limits for occupationally exposed workers as well as members of the public are not exceeded through an effective regulatory control by authorisations and inspections of all dosimetry laboratories and end user institutions.

Technical assistance and codes of practice should be provided to these laboratories in metrology and calibration issues to fulfil the legal requirement under the Radiation Protection Instrument of the country and also contribute to the education of staff and members of the public in metrology of ionizing radiation.

The Regulatory Authority should also enforce regular calibration of all end user instruments so as to meet the international safety requirements and put in place mechanisms which will ensure that serious deterioration in equipment, operational procedures or management controls are promptly corrected.

5.2.3 End User Institutions

The End User institution has the primary responsibility of safety of its facility or activity. They are to ensure that all ionising radiation measuring instruments are calibrated annually or after major repair so that they give accurate and correct reading with acceptable uncertainties.

The institutions must also ensure that occupational doses are kept as low as reasonably achievable (ALARA) taken into consideration social and economic factors. They should also develop a comprehensive Radiation Protection Programme (RPP) which includes recalibration at regular intervals and must be supported with a policy level commitment.

Periodic training of workers should be put in place and a qualified Radiation Protection Officer (RPO) charged with the responsibility of radiation protection and safety of radiation sources should be officially appointed.

REFERENCES

Adjei D, Darko E. O, Schandorf C, Owusu-Manteaw P and Akrobortu E. (2012).Personal dose analysis of TLD glow curve data from individual monitoring records. Oxford Journal of Radiation Protection Dosimetry. 152(4), 273–278.

Adjei D, Darko E. O, Annkah J. K, Amoako J. K, Ofori K, Emi-Reynolds G, Obeng M. K, Akomaning-Adofo E, Owusu-Manteaw P. (2013). Analysis of Calibration Results of Radiation Survey Meters used for area Monitoring. Retrieved from http://rpd.oxfordjournals.org on 8th April 2013.

Annkah J. K, Darko E. O, Amoako J. K, Emi-Reynolds G, Obeng M. K, Royle G. (2011). Preliminary investigations of the contribution of scatter radiation during calibration for TLD-100 using a Cs-137 panoramic source. Research Journal of Applied Sciences, Engineering and Technology 3(9): 874–879, 2011.

Arwui C.C, Deatanyah P, Wotorchi-Gordon S, Ankaah J, Emi-Reynolds J.G, Amoako J.K, Adu S, Obeng M, Hasford F, Lawluvi H, Kpeglo D.O, Sosu E.K (2011). Assessment of the Effectiveness of Collimation of ^{137}Cs Panoramic Beam on TLD Calibration Using a Constructed Lead Block Collimator and an ICRU Slab Phantom at SSDL in Ghana. International Journal of Science and Technology.Volume 1 No. 4, Pp169-173.

BIPM, IEC, IFCC, ISO, IUPAC, IUPAP, and OIML. Guide to the expression of uncertainty in measurement. International Organization for Standardization (1995).

Bohm J, Alberts, W. G, Swinth K. L, Soares C. G, McDonald J. C, Thompson I.M.G, Kramer H. M. (1999). ISO recommended reference radiations for the calibration and proficiency testing of dosimeters and dose rate meters used in radiation protection. Rad. Prot. Dosim. 86, 87-105.

Carlsson C. A, Alm C. G, Lund E, Matscheko G, Pettersson H. L. B. (1996).An instrument for measuring ambient dose equivalent, H (10).Radiat Prot Dosim 67(1):33–39

Cember H, Johnson T. E. (2009).Introduction to Health Physics, 4th edition, The McGraw-Hill Companies, Inc. New York, pp209-210, 218-221.

Charlie C. M. (2009). Kilovoltage X-ray Dosimetry for Radiation Therapy. AAPM Summer School, pp.21-25.

Chidal K, Nishimura Y, Sato Y, Endo A, Sakamoto M, Hoshi C, Zuguchi M. (2008). Examination of the long-term stability of radiation survey meters and electronic pocket dosemeters. Radiation Protection Dosimetry. 129(4), 431–434.

De Freitas L. C, Drexler G (1992). The role of secondary standard dosimetry laboratories in diagnostic radiology. Radiation Protection Dosimetry. 43(1–4), 99–102.

European Co-operation for Accreditation, (1999).Expression of the Uncertainty of Measurement in Calibration, EA-4/02 pp.6-10.

Horowitz, Y.R., 1990. Study of the Annealing Characteristics of Li Mg, Ti using Computerised Glow Curve Deconvolution Radiation Protection Dosimetry,33: 255-258.

IAEA, (1996).International Basic Safety Standards for Protection against Ionizing Radiation and for the Safety of Radiation Sources. International Atomic Energy Agency, Vienna, Safety Series No. 115.

IAEA, (1999).SSDL News Letters. No. 41 IAEA/WHO Network of Secondary Standard Dosimetry Laboratories. International Atomic Energy Agency, Vienna, pp.13-14.

IAEA, (2000).Calibration of radiation protection monitoring instruments. International Atomic Energy Agency, Vienna, Safety Reports Series No. 16, pp.1-21.

IAEA, (2000).Absorbed Dose Determination in External Beam Radiotherapy. An International Code of Practice for Dosimetry Based on Standards of Absorbed Dose to Water. International Atomic Energy Agency, Vienna, Technical Report Series No. 398 pp. 6-7.

IAEA, (2005). Radiation Oncology Physics: A Handbook for Teachers and Students. International Atomic Energy Agency, Vienna, pp.5-48.

IAEA, (2007).Dosimetry in Diagnostic Radiology: An International Code of Practice. International Atomic Energy Agency, Vienna, Technical Report Series No. 457, pp.82.

IAEA, (2008). Measurement Uncertainty: A Practical Guide For Secondary Standards Dosimetry Laboratories. International Atomic Energy Agency, Vienna, TECDOC.No.1585 pp.1-44.

IAEA, (2009).Calibration of Reference Dosimeters for External Beam Radiotherapy. International Atomic Energy Agency, Vienna, Technical Reports Series No.469, pp. 8, 21-28, 59-67, 120.

ICRP (1991).The 1990 recommendations of the International Commission on Radiological Protection. International Commission on Radiological Protection, Publication 60.Ann ICRP 21(1–3). Pergamon Press, Oxford.

ICRP (2007).The 2007 recommendations of the International Commission on Radiological Protection. International Commission on Radiological Protection, Publication 103. Ann ICRP 37(2–4). Pergamon Press, Oxford.

ICRU (1998).Conversion coefficients for use in radiological protection against externalradiation. International Commission on Radiation Units and Measurements, Report 57, Bethesda.

ISO (1996).X and gamma reference radiation for calibrating dosimeters and dose rate meters and for determining their response as a function of photon energy. Part 1: Radiation characteristics and production methods. International Organisation for Standardisation, ISO 4037-1.

ISO (1997).X and gamma reference radiation for calibrating dosimeters and dose rate meters and for determining their response as a function of photon energy. Part 2:

Dosimetry for radiation protection over the energy ranges from 8 keV to 1.3 MeV and 4 MeV to 9 MeV. International Organisation for Standardisation, ISO 4037-2.

ISO (1999). X and gamma reference radiation for calibrating dosimeters and dose rate meters and for determining their response as a function of photon energy. Part 3: Calibration of area and personal dosimeters and the measurement of their response as a function of energy and angle of incidence. International Organisation for Standardisation, ISO 4037-3.

ISO (2005).General Requirements for the Competence of Testing and Calibration Laboratories. International Organisation for Standardisation Geneva, ISO/IEC 17025.

Jozela S. (2007). Beam Quality Specification in kilo-voltage radiotherapy. Master of Science thesis. University of the Witwatersrand, Johannesburg, pp.3.

Khalil M. M. (2001). Basic Sciences of Nuclear Medicine. Springer-Verlag Berlin Heidelberg, Pp.11.

Knoll, G.F.(2000). Radiation Detection and Measurement, 3rd edition, John Wiley & Sons, Inc. New York, pp. 48-52, 58-64.

Kramers H. M. (1992). European intercomparison of diagnostic dosemeters: calibration of the reference dosemters. Radiation Protection Dosimetry. 43(1–4), 75–79.

Lamarsh J. R, Baratta A. J. (2001). Introduction to Nuclear Engineering. Third Edition. Prentice-Hall, Inc. Upper Saddle River, New Jersey, pp. 3,91-100.

Lewis V, Woods M, Burgess P, Green S, Simpson J, Wardle J. (2003). The Assessment of Uncertainty in Radiological Calibration and Testing. Measurement Good Practice Guide No. 49, ISSN: 1368-6550. pp. 3-16.

Ma C. M, Coffey C. W, Dewerd L. A, Liu C, Nath R, Seitzer S. M, Seuntjens J. P. (2001). AAPM protocol for 40-300 kV x-ray beam dosimetry in radiotherapy and radiobiology. Medical physics, vol. 26, No.6, pp.872

Martin J. E (2006). Physics for Radiation Protection: A Handbook. Second Edition, Completely Revised and Enlarged WILEY-VCH Verlag GmbH & Co. KGaA, Weinheim, pp.307-336, 577.

McDonald J. C(2004).Calibration measurements and standards for radiation protection dosimetry. Radiation Protection Dosimetry. 109(4), 317–321.

Piesch E. (1981). Application of TLD Systems for Environmental Monitoring. In: Oberhofer, M. and A. Scharmann, (Eds.), Applied Thermoluminescence Dosimetry. Adam Hilgar, Bristol, pp. 197-228.

Roberson P.L, Carlson R. D. (1992). Determining the lower limit of detection for personnel dosimetry systems. Health Phys., 62(1): 2-9.

Sabol J, Weng P. S. (1995).Introduction to radiation protection dosimetry.World Scientific, Singapore pp.1-2.

Seibert J. A, Boone J. M. (2005).X-Ray Imaging Physics for Nuclear Medicine Technologists. Part 2: X-Ray Interactions and Image Formation. Journal of Nuclear Medicine Technology, pp.3-18.

Shapiro J. (2002). Radiation Protection: A guide for Scientists, Regulators and Physicians, 4th edition Harvard University Press, England, pp.7-8.

Smith F. A(2000). A Primer in Applied Radiation Physics, World Scientific Publishing Co Ltd, Country, pp: 6-15, 257-259, 102-103.

Stadtmann H (2001). Dose quantities in radiation protection and dosimeter calibration. Radiation Protection Dosimetry. 96 (1-3), 21-26.

Suliman I.I, Youssif B.E, Beineen A.A, Suliman M.H (2010). Calibration of radiation protection area monitoring instruments in Sudan, pp.1-4.

Tuner J. E. (2007).Atoms, Radiation and Radiation Protection. Third, completely revised and enlarged edition. Wiley-VCH Verlag GmbH and Co KGaA, pp.173-200, 262.

APPENDICES

APPENDIX 1

ATTENUATION CURVES FOR 80 kV to 250 kV FROM WHICH THE HVL WAS DETERMINED

The attenuation curve generated for 80 kV radiation is shown in Figure 1A.

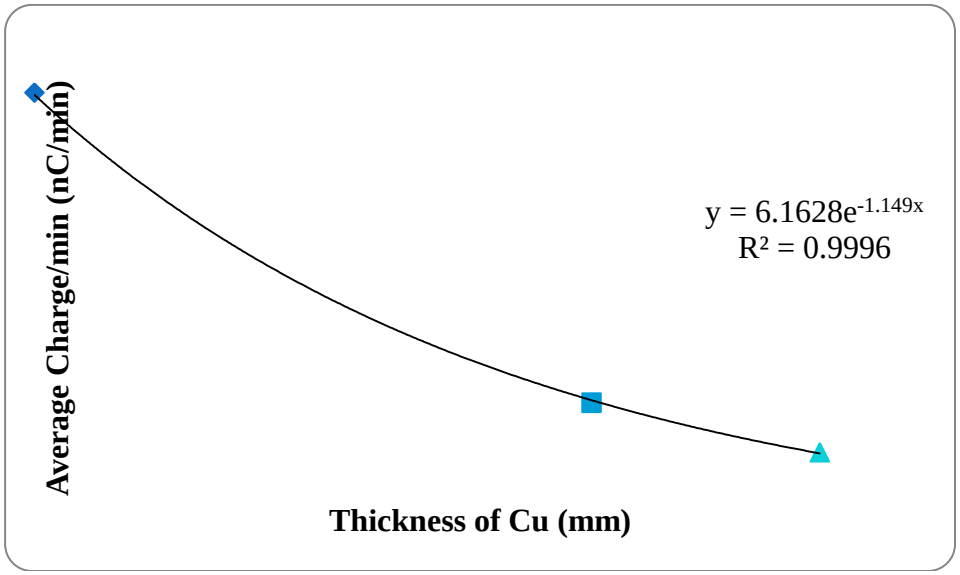

Figure 1A: Attenuation curve generated for 80 kV

The attenuation curve generated for 100 kV radiation is shown in Figure 1B.

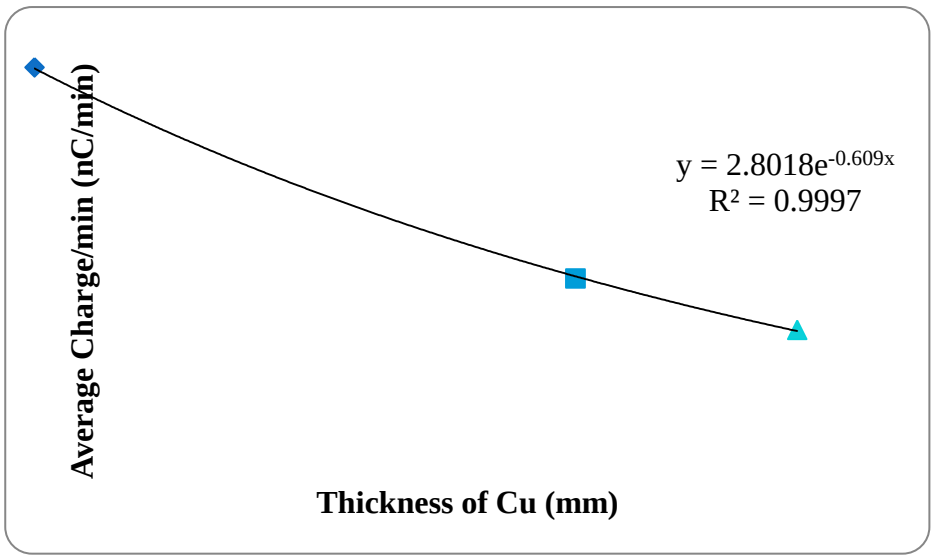

Figure 1B: Attenuation curve generated for 100 kV

The attenuation curve generated for 150 kV radiation is shown in Figure 1C.

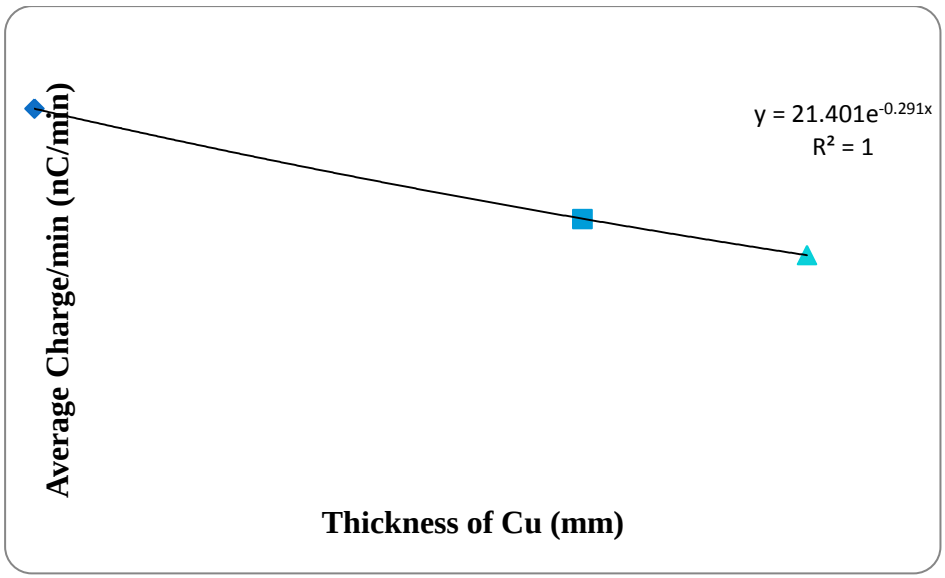

Figure 1C: Attenuation curve generated for 150kV

The attenuation curve generated for 200 kV radiation is shown in Figure 1D.

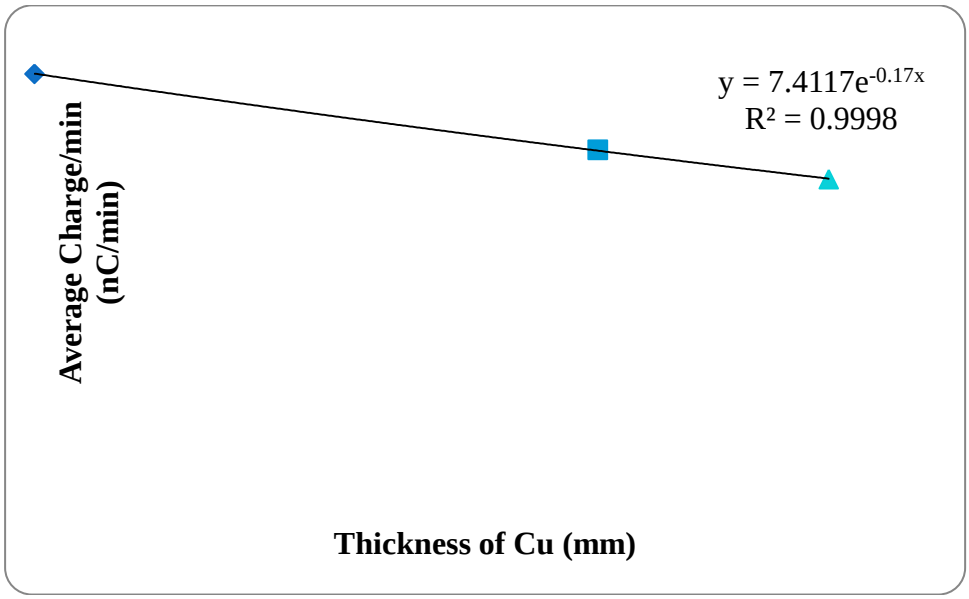

Figure 1D: Attenuation curve generated for 200kV

The attenuation curve generated for 250 kV radiation is shown in Figure 1E.

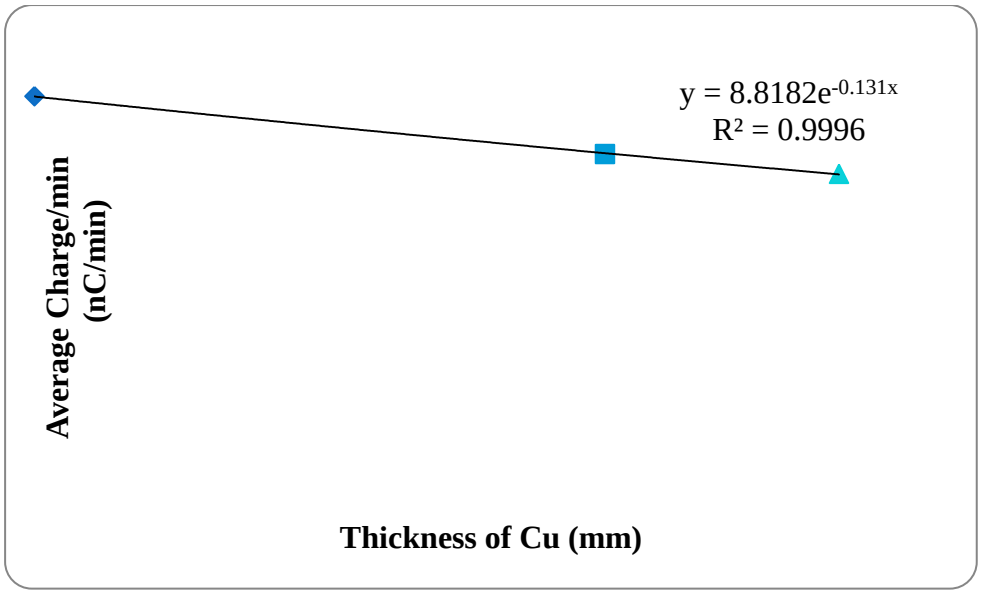

Figure 1E: Attenuation curve generated for 250 Kv

APPENDIX 2

Table 2 A: Charges measured at 1m from X-ray unit

No.	60 kV,10 mA		80 kV,10 mA		100 kV,10 mA		150 kV,10 mA		200 kV,10 mA		250 kV,10 mA	
	Leakage Reading (nC)	Exposure Reading (nC)	Leakage Reading (nC)	Exposure Reading (nC)	Leakage Reading (nC)	Exposure Reading (nC)	Leakage Reading (nC)	Exposure Reading (nC)	Leakage Reading (nC)	Exposure Reading (nC)	Leakage Reading (nC)	Exposure Reading (nC)
1	0.1260	10.8900	0.0950	7.8810	0.0970	3.5230	0.1030	28.2400	0.0760	9.5650	0.0960	7.3090
2	0.1050	11.4100	0.0920	7.9050	0.0670	5.5220	0.0950	29.3500	0.0950	9.9720	0.0990	8.0150
3	0.1140	11.0900	0.0990	8.0320	0.0980	3.6090	0.0840	28.7900	0.0910	10.0800	0.0910	8.2200
4	0.1010	11.2700	0.1010	8.0320	0.1090	3.6380	0.0990	29.0100	0.1030	9.8860	0.1020	8.0030
5	0.0970	11.3700	0.1050	7.9940	0.1130	3.5120	0.0790	28.5400	0.1160	10.0800	0.1050	7.9680
6	0.1210	11.0800	0.0980	7.9980	0.0870	3.5210	0.1090	28.9900	0.0970	9.7620	0.1110	7.6520
7	0.0890	10.8900	0.0930	7.8620	0.0890	3.5060	0.0970	28.8700	0.0840	10.0500	0.0950	7.9980
8	0.0990	10.8800	0.0920	8.0150	0.0720	3.5090	0.0850	29.0200	0.0920	10.0200	0.0880	8.0340
9	0.0750	11.0200	0.0990	8.0220	0.0830	3.5220	0.0990	29.0500	0.0890	9.9850	0.0930	8.0250
10	0.0880	11.2600	0.0870	7.9240	0.0870	3.5060	0.0910	29.1300	0.0950	10.0800	0.0990	8.1090
Average	0.1015	11.1160	0.0961	7.9665	0.0902	3.5368	0.0941	28.8990	0.0938	9.9480	0.0979	7.9333
Corrected Exposure Reading	11.0145 nC		7.8704 nC		3.4466 nC		28.8049 nC		9.8542 nC		7.8354 nC	

Table 2 B: Charges measured at 1.5 m from X-ray unit

No.	60 kV,10 mA		80 kV,10 mA		100 kV,10 mA		150 kV,10 mA		200 kV,10 mA		250 kV,10 mA	
	Leakage Reading (nC)	Exposure Reading (nC)	Leakage Reading (nC)	Exposure Reading (nC)	Leakage Reading (nC)	Exposure Reading (nC)	Leakage Reading (nC)	Exposure Reading (nC)	Leakage Reading (nC)	Exposure Reading (nC)	Leakage Reading (nC)	Exposure Reading (nC)
1	0.1130	5.0730	0.1030	3.8520	0.0930	2.0240	0.0980	12.8530	0.1050	4.4450	0.1070	4.1330
2	0.0850	5.1020	0.1080	3.6870	0.0950	2.0540	0.0850	12.7660	0.0780	4.4780	0.0950	4.1500
3	0.0940	4.9960	0.0920	3.7570	0.0840	2.0340	0.0840	12.7580	0.0820	4.4430	0.0930	4.1020
4	0.1210	5.0150	0.1010	3.8320	0.1010	2.0110	0.1070	12.6920	0.1010	4.4580	0.0790	4.1110
5	0.1090	5.0020	0.1050	3.7761	0.1190	2.0060	0.1140	12.5970	0.1080	4.3920	0.0890	3.9860
6	0.0910	4.9880	0.0930	3.8600	0.0970	2.1040	0.0890	12.7320	0.1090	4.4390	0.0870	4.1090
7	0.0750	4.8100	0.0850	3.6720	0.0850	2.0570	0.0850	12.8250	0.0960	4.2870	0.0960	4.1260
8	0.0620	5.2010	0.0870	3.7290	0.0820	2.0190	0.0770	12.6730	0.0770	4.3690	0.0930	4.1580
9	0.0690	5.0100	0.0920	3.7860	0.0780	2.1180	0.0840	12.8860	0.0790	4.3750	0.0920	4.1070
10	0.0930	5.0200	0.0930	3.8250	0.0910	2.1120	0.0830	12.9640	0.0840	4.2850	0.0970	4.1250
Average	0.0912	5.0217	0.0959	3.7776	0.0925	2.0539	0.0906	12.7746	0.0919	4.3971	0.0928	4.1107
Corrected Exposure Reading	4.9305 nC		3.6817 nC		1.9614 nC		12.684 nC		4.3052 nC		4.0179 nC	

Table 2 C: Charges measured at 2 m from X-ray unit

No.	60 kV,10 mA		80 kV,10 mA		100 kV,10 mA		150 kV,10 mA		200 kV,10 mA		250 kV,10 mA	
	Leakage Reading (nC)	Exposure Reading (nC)	Leakage Reading (nC)	Exposure Reading (nC)	Leakage Reading (nC)	Exposure Reading (nC)	Leakage Reading (nC)	Exposure Reading (nC)	Leakage Reading (nC)	Exposure Reading (nC)	Leakage Reading (nC)	Exposure Reading (nC)
1	0.1080	3.1100	0.0980	2.1980	0.0980	1.9375	0.1080	8.2320	0.1090	3.5200	0.0930	2.2180
2	0.1250	3.1890	0.1050	2.1180	0.0950	1.8775	0.0950	8.2250	0.0850	3.5920	0.0790	2.2340
3	0.0760	3.2790	0.0850	2.3750	0.0890	1.8680	0.0990	8.2380	0.0950	3.4810	0.0960	2.1490
4	0.0930	3.0110	0.1060	2.1170	0.0820	1.8029	0.1010	8.2570	0.0840	3.4250	0.0970	2.2450
5	0.1020	3.0150	0.1140	2.1380	0.0990	1.8652	0.1050	8.2240	0.0890	3.3980	0.0890	2.2060
6	0.1050	3.1350	0.0990	2.1940	0.1010	1.8870	0.0970	8.2390	0.0990	3.4010	0.0960	2.1780
7	0.0970	3.2800	0.0870	2.1760	0.0980	1.9015	0.0820	8.2470	0.0970	3.3680	0.0850	2.1930
8	0.0780	3.1220	0.0760	2.2090	0.0950	1.9342	0.0920	8.2280	0.0820	3.3790	0.0960	2.2250
9	0.0830	3.1370	0.0890	2.1420	0.0890	1.9260	0.0850	8.2570	0.0990	3.4120	0.0880	2.2110
10	0.0870	3.125	0.0990	2.2010	0.0970	1.9823	0.0890	8.3610	0.0960	3.5680	0.0890	2.1950
Average	0.0954	3.1403	0.0958	2.1868	0.0943	1.8982	0.0953	8.2508	0.0935	3.4544	0.0908	2.2054
Corrected Exposure Reading	3.0449 nC		2.0910nC		1.8039 nC		8.1555 nC		3.3609 nC		2.1146 nC	

Table 2 D: Charges measured at 2.5 m from X-ray unit

No.	60 kV,10 mA		80 kV,10 mA		100 kV,10 mA		150 kV,10 mA		200 kV,10 mA		250 kV,10 mA	
	Leakage Reading (nC)	Exposure Reading (nC)	Leakage Reading (nC)	Exposure Reading (nC)	Leakage Reading (nC)	Exposure Reading (nC)	Leakage Reading (nC)	Exposure Reading (nC)	Leakage Reading (nC)	Exposure Reading (nC)	Leakage Reading (nC)	Exposure Reading (nC)
1	0.0880	2.2140	0.0930	2.0680	0.1120	1.4680	0.0980	5.1720	0.1010	2.1560	0.1050	2.0060
2	0.1070	2.1980	0.0970	2.0910	0.0880	1.4890	0.0950	5.1580	0.0960	2.1860	0.0940	1.7690
3	0.0830	2.2140	0.0990	2.1050	0.0960	1.4750	0.0920	5.1630	0.0840	2.1630	0.0870	1.9820
4	0.1140	2.1360	0.1090	2.1080	0.0780	1.4220	0.1080	5.1850	0.0880	2.1480	0.0780	1.9950
5	0.1120	2.1100	0.1010	2.0760	0.0890	1.4450	0.0870	5.1770	0.0910	2.2030	0.0740	2.0120
6	0.1210	2.0060	0.0970	2.0640	0.0950	1.4532	0.0880	5.1890	0.0990	2.1770	0.0990	2.0580
7	0.1090	2.1150	0.1080	2.1010	0.0990	1.4390	0.0950	5.1670	0.0760	2.1930	0.0830	2.0340
8	0.0650	2.1280	0.0850	2.0870	0.0850	1.5020	0.0860	5.1550	0.0960	2.1640	0.0880	2.0160
9	0.0820	2.2450	0.0880	2.1060	0.0880	1.4760	0.0910	5.1720	0.0870	2.1450	0.0940	2.0010
10	0.0850	2.1160	0.0860	2.0820	0.0830	1.4420	0.0970	5.1880	0.0890	2.1880	0.0960	2.0170
Average	0.0966	2.1482	0.0963	2.0888	0.0913	1.4611	0.0937	5.1726	0.0907	2.1723	0.0898	1.9890
Corrected Exposure Reading	2.0516 nC		1.9925 nC		1.3698 nC		5.0789 nC		2.0816 nC		1.8992 nC	

Table 2 E: Charges measured at 3 m from X-ray unit

No.	60 kV,10 mA		80 kV,10 mA		100 kV,10 mA		150 kV,10 mA		200 kV,10 mA		250 kV,10 mA	
	Leakage Reading (nC)	Exposure Reading (nC)	Leakage Reading (nC)	Exposure Reading (nC)	Leakage Reading (nC)	Exposure Reading (nC)	Leakage Reading (nC)	Exposure Reading (nC)	Leakage Reading (nC)	Exposure Reading (nC)	Leakage Reading (nC)	Exposure Reading (nC)
1	0.1100	2.0320	0.0860	1.5850	0.1020	1.0937	0.1050	4.1330	0.0930	1.7150	0.1020	1.4380
2	0.1060	1.9870	0.0810	1.5590	0.0950	1.0884	0.0770	4.1470	0.1080	1.7020	0.0780	1.4690
3	0.1130	1.9630	0.0880	1.6870	0.0940	1.0913	0.0970	4.2780	0.0950	1.7110	0.0820	1.4930
4	0.0975	2.0090	0.0910	1.5420	0.0980	1.0567	0.0910	4.0280	0.1020	1.7800	0.0910	1.5020
5	0.0840	2.2110	0.0990	1.5530	0.1050	1.1002	0.1080	4.0970	0.1150	1.7220	0.0890	1.4510
6	0.1130	2.0130	0.0910	1.6010	0.0950	1.0998	0.0910	4.1260	0.0970	1.7040	0.0910	1.5030
7	0.0850	2.0400	0.0870	1.6110	0.0830	1.0764	0.0850	4.1380	0.0990	1.6590	0.0880	1.4970
8	0.0920	2.0980	0.0920	1.6090	0.0770	1.0952	0.0980	4.1220	0.0920	1.7120	0.0930	1.4650
9	0.0770	2.0870	0.0990	1.5520	0.0690	1.0987	0.0990	4.2090	0.0970	1.6650	0.0940	1.4860
10	0.0780	2.0100	0.0950	1.5480	0.0930	1.0994	0.0860	4.2110	0.0850	1.7340	0.0970	1.5320
Average	0.0956	2.0450	0.0909	1.5847	0.0911	1.0900	0.0937	4.1489	0.0983	1.7104	0.0905	1.4836
Corrected Exposure Reading	1.9495 nC		1.4938 nC		0.9989 nC		4.0552 nC		1.6121 nC		1.3931 nC	

Table 2 F: Charges measured at 3.5 m from X-ray unit

No.	60 kV,10 mA		80 kV,10 mA		100 kV,10 mA		150 kV,10 mA		200 kV,10 mA		250 kV,10 mA	
	Leakage Reading (nC)	Exposure Reading (nC)	Leakage Reading (nC)	Exposure Reading (nC)	Leakage Reading (nC)	Exposure Reading (nC)	Leakage Reading (nC)	Exposure Reading (nC)	Leakage Reading (nC)	Exposure Reading (nC)	Leakage Reading (nC)	Exposure Reading (nC)
1	0.1030	1.5780	0.1010	1.4690	0.1070	0.8540	0.1070	3.3060	0.1010	1.3680	0.0930	1.2240
2	0.0960	1.4970	0.0770	1.4630	0.0850	0.8260	0.1080	3.3010	0.0780	1.3470	0.0940	1.2260
3	0.0810	1.5580	0.0930	1.4380	0.0990	0.8440	0.0950	3.3110	0.0890	1.3330	0.0860	1.3450
4	0.0970	1.4990	0.1090	1.4850	0.1010	0.8560	0.0980	3.3050	0.1070	1.3980	0.0880	1.2360
5	0.1050	1.5230	0.1160	1.5020	0.0990	0.8720	0.1050	3.3060	0.1090	1.3460	0.0970	1.2950
6	0.1010	1.5320	0.0980	1.5230	0.0810	0.8625	0.0950	3.3130	0.0860	1.4050	0.0940	1.2840
7	0.1030	1.5860	0.0950	1.4590	0.0750	0.8794	0.0920	3.3170	0.0770	1.3520	0.0810	1.3360
8	0.0760	1.5690	0.0880	1.4800	0.0850	0.8423	0.0820	3.3280	0.0830	1.3320	0.0930	1.2670
9	0.0910	1.5220	0.0840	1.4120	0.0990	0.8515	0.0970	3.3040	0.0870	1.3480	0.0850	1.2910
10	0.0820	1.5830	0.0910	1.4070	0.0830	0.8626	0.0830	3.3050	0.0880	1.3920	0.0960	1.3110
Average	0.0935	1.5447	0.0952	1.4638	0.0914	0.8550	0.0962	3.3096	0.0905	1.3621	0.0907	1.2815
Corrected Exposure Reading	1.4512 nC		1.3686 nC		0.7636 nC		3.2134 nC		1.2716 nC		1.1908 nC	

Table 2 G: Charges measured at 4 m from X-ray unit

No.	60 kV,10 mA		80 kV,10 mA		100 kV,10 mA		150 kV,10 mA		200 kV,10 mA		250 kV,10 mA	
	Leakage Reading (nC)	Exposure Reading (nC)	Leakage Reading (nC)	Exposure Reading (nC)	Leakage Reading (nC)	Exposure Reading (nC)	Leakage Reading (nC)	Exposure Reading (nC)	Leakage Reading (nC)	Exposure Reading (nC)	Leakage Reading (nC)	Exposure Reading (nC)
1	0.1120	1.3960	0.0930	1.1453	0.1050	0.7130	0.1110	2.0750	0.0830	1.0250	0.1060	0.6470
2	0.1070	1.3890	0.0870	1.1280	0.1080	0.6990	0.1080	2.0931	0.0980	1.0750	0.0780	0.6220
3	0.0990	1.3623	0.0940	1.1490	0.1120	0.6980	0.1090	2.0548	0.0990	1.0120	0.0920	0.6410
4	0.0720	1.3550	0.1010	1.2050	0.1060	0.7020	0.1220	2.0321	0.0920	1.0810	0.0860	0.6590
5	0.1090	1.3963	0.0890	1.1260	0.0890	0.7115	0.1080	2.0762	0.0890	1.0060	0.0890	0.6120
6	0.1010	1.3921	0.0880	1.1350	0.0950	0.7060	0.0930	2.0826	0.0920	1.0350	0.0970	0.6870
7	0.0830	1.3290	0.0970	1.1380	0.0850	0.7125	0.0950	2.0543	0.0970	1.0230	0.0850	0.6910
8	0.0810	1.3260	0.0920	1.1160	0.0860	0.7180	0.0920	2.0850	0.1060	1.0020	0.0820	0.6730
9	0.0830	1.3550	0.0890	1.1250	0.0990	0.7260	0.0890	2.0997	0.0910	1.0150	0.0890	0.6620
10	0.0910	1.3256	0.0930	1.1276	0.0970	0.7330	0.0960	2.0995	0.0860	1.0320	0.0988	0.6650
Average	0.0938	1.3626	0.0923	1.1395	0.0982	0.7119	0.1023	2.0752	0.0933	1.0306	0.0903	0.6559
Corrected Exposure Reading	1.2688 nC		1.0472 nC		0.6137 nC		1.9729 nC		0.9373 nC		0.5656 nC	

Table 2 H: Charges measured at 4.5 m from X-ray unit

No.	60 kV,10 mA		80 kV,10 mA		100 kV,10 mA		150 kV,10 mA		200 kV,10 mA		250 kV,10 mA	
	Leakage Reading (nC)	Exposure Reading (nC)	Leakage Reading (nC)	Exposure Reading (nC)	Leakage Reading (nC)	Exposure Reading (nC)	Leakage Reading (nC)	Exposure Reading (nC)	Leakage Reading (nC)	Exposure Reading (nC)	Leakage Reading (nC)	Exposure Reading (nC)
1	0.0980	1.1370	0.0790	0.8130	0.1150	0.6790	0.1090	1.8240	0.1030	0.8934	0.1020	0.3770
2	0.1030	1.1320	0.0820	0.8740	0.0950	0.6690	0.0880	1.7590	0.1080	0.8762	0.0920	0.3980
3	0.0820	1.1210	0.0960	0.8020	0.0860	0.6450	0.0890	1.8230	0.1010	0.8576	0.0870	0.4080
4	0.0760	1.1350	0.1120	0.8110	0.1210	0.6310	0.1070	1.7620	0.0960	0.8871	0.0930	0.3760
5	0.0950	1.1070	0.1050	0.8096	0.1090	0.6580	0.1120	1.7830	0.1030	0.8955	0.0990	0.3850
6	0.1120	1.1280	0.0960	0.8083	0.0890	0.6440	0.0990	1.7840	0.0970	0.8532	0.0940	0.3910
7	0.1010	1.1170	0.0850	0.8055	0.0950	0.6490	0.0870	1.8430	0.0990	0.8675	0.0880	0.3540
8	0.0860	1.1360	0.0770	0.8155	0.0820	0.6570	0.0780	1.7920	0.0850	0.8997	0.0850	0.3650
9	0.0940	1.1280	0.0930	0.7982	0.0790	0.6680	0.0930	1.8770	0.0990	0.9004	0.0910	0.3820
10	0.0930	1.1350	0.0940	0.7826	0.0980	0.6710	0.0870	1.8950	0.0970	0.8915	0.0970	0.4110
Average	0.0940	1.1276	0.0919	0.8120	0.0969	0.6571	0.0949	1.8142	0.0988	0.8822	0.0928	0.3847
Corrected Exposure Reading	1.0336 nC		0.7201 nC		0.5602 nC		1.7193 nC		0.7834 nC		0.2919 nC	

Table 2 I: Charges measured at 5 m from X-ray unit

No.	60 kV,10 mA		80 kV,10 mA		100 kV,10 mA		150 kV,10 mA		200 kV,10 mA		250 kV,10 mA	
	Leakage Reading (nC)	Exposure Reading (nC)	Leakage Reading (nC)	Exposure Reading (nC)	Leakage Reading (nC)	Exposure Reading (nC)	Leakage Reading (nC)	Exposure Reading (nC)	Leakage Reading (nC)	Exposure Reading (nC)	Leakage Reading (nC)	Exposure Reading (nC)
1	0.1150	1.0060	0.1150	0.7130	0.1050	0.5226	0.1120	1.1560	0.0930	0.6470	0.1070	0.3010
2	0.0780	0.9970	0.0990	0.7430	0.0850	0.5210	0.0950	1.1280	0.0950	0.6870	0.0950	0.2870
3	0.0760	1.0150	0.0980	0.7150	0.0740	0.5388	0.0970	1.1190	0.0820	0.6730	0.0890	0.2990
4	0.0780	1.0620	0.1050	0.7260	0.0910	0.5411	0.0810	1.1480	0.0880	0.6460	0.0960	0.3120
5	0.1120	1.0080	0.0990	0.7330	0.0980	0.5290	0.1040	1.1550	0.0970	0.6450	0.0890	0.3180
6	0.1140	1.0020	0.1040	0.7290	0.0910	0.5211	0.0860	1.1430	0.0950	0.6780	0.0950	0.3040
7	0.1070	1.0230	0.0950	0.6980	0.0880	0.5364	0.0950	1.1590	0.0850	0.6430	0.0970	0.2860
8	0.0980	0.9980	0.1030	0.6990	0.0930	0.5319	0.0870	1.1760	0.0920	0.6330	0.0890	0.2930
9	0.0760	0.9920	0.0980	0.6780	0.0890	0.5125	0.0990	1.1582	0.0960	0.6170	0.0960	0.3160
10	0.0790	1.0040	0.0910	0.6880	0.0870	0.5116	0.0960	1.2030	0.0910	0.6780	0.0920	0.3070
Average	0.0933	1.0107	0.1007	0.7122	0.0901	0.5266	0.0952	1.1545	0.0914	0.6547	0.0945	0.3023
Corrected Exposure Reading	0.9174 nC		0.6115 nC		0.4365 nC		1.0593 nC		0.5633 nC		0.2078 nC	

Table 2 J: Charges measured at 1m to 3 m from ^{137}Cs gamma irradiator

No.	Reference distance 1.0 m		Reference distance 1.5 m		Reference distance 2.0 m		Reference distance 2.5 m		Reference distance 3.0 m	
	Leakage Reading (nC)	Exposure Reading (nC)	Leakage Reading (nC)	Exposure Reading (nC)	Leakage Reading (nC)	Exposure Reading (nC)	Leakage Reading (nC)	Exposure Reading (nC)	Leakage Reading (nC)	Exposure Reading (nC)
1	0.1035	2.2130	0.1015	0.8230	0.0915	0.8335	0.0905	0.5895	0.0800	0.5080
2	0.1110	2.2010	0.0985	0.8095	0.0950	0.6695	0.0855	0.5435	0.0675	0.5610
3	0.0970	2.2160	0.0950	0.8885	0.0895	0.6630	0.0880	0.5535	0.0805	0.5045
4	0.1005	2.1790	0.0955	0.8985	0.0880	0.7235	0.0860	0.5185	0.0820	0.5835
5	0.1020	2.1220	0.0985	0.9005	0.0895	0.7365	0.0875	0.5775	0.0795	0.5655
6	0.1075	2.1080	0.0930	0.9060	0.0880	0.8510	0.0865	0.5435	0.0755	0.4550
7	0.1060	2.0800	0.1005	0.9255	0.0950	0.7675	0.0870	0.6320	0.0855	0.5040
8	0.1080	2.0340	0.0915	0.9965	0.0905	0.8410	0.0805	0.5725	0.0830	0.5300
9	0.1070	2.1130	0.0890	1.0425	0.0955	0.8055	0.0780	0.6120	0.0865	0.5310
10	0.1080	2.1710	0.0835	0.9810	0.0875	0.8635	0.0850	0.5165	0.0795	0.5335
Average	0.1051	2.1437	0.0947	0.9172	0.0910	0.7755	0.0855	0.5659	0.0800	0.5276
Corrected Exposure Reading	2.0387nC		0.8225 nC		0.6845 nC		0.48045 nC		0.4477nC	

Table 2 K: Charges measured at 3.5 m to 5 m from ^{137}Cs gamma irradiator

No.	Reference distance 3.5 m		Reference distance 4.0 m		Reference distance 4.5 m		Reference distance 5.0 m	
	Leakage Reading (nC)	Exposure Reading (nC)	Leakage Reading (nC)	Exposure Reading (nC)	Leakage Reading (nC)	Exposure Reading (nC)	Leakage Reading (nC)	Exposure Reading (nC)
1	0.0805	0.477	0.0710	0.3935	0.0700	0.3185	0.0770	0.3075
2	0.0735	0.490	0.0725	0.4870	0.0725	0.3845	0.0655	0.2985
3	0.0600	0.5545	0.0675	0.4850	0.0670	0.3800	0.0590	0.2675
4	0.0580	0.5535	0.0605	0.3775	0.0605	0.3330	0.0730	0.3070
5	0.0695	0.5025	0.0680	0.4490	0.0620	0.3480	0.0520	0.2905
6	0.0775	0.5345	0.0695	0.3435	0.0610	0.3195	0.0720	0.2745
7	0.0760	0.5460	0.0600	0.5005	0.0710	0.3610	0.0690	0.2675
8	0.0785	0.5190	0.0615	0.4860	0.0645	0.3275	0.0635	0.2830
9	0.0705	0.5360	0.0625	0.4145	0.0630	0.3115	0.0575	0.2855
10	0.0700	0.4470	0.0625	0.4075	0.0610	0.3185	0.0620	0.2725
Average	0.0714	0.5160	0.0656	0.4344	0.0653	0.3402	0.0651	0.2854
Corrected Exposure Reading	0.4446 nC		0.3689nC		0.2750nC		0.2204nC	

APPENDIX 3

Table 3 A: Calibration certificate for SSDL reference instrument

International Atomic Energy Agency

Calibration certificate No. GHA/2007/03

The following instruments from ***Ghana Atomic Energy Commission, Radiation Protection Institute Legon, Accra***

have been calibrated at the IAEA Dosimetry Laboratory:

	Ionization chamber	Electrometer
Model/type:	*LS-01*	*UNIDOS*
Serial number:	*227*	*20243*
Manufacturer:	*PTW Freiburg*	*PTW Freiburg*
Calibration period:	from *2007-Apr-05*	to *2007-Jun-12*

Calibration coefficients in terms of air kerma

The calibrations have been performed following the procedure given in Appendix 3B "Ionization Chamber Calibration Procedures at the IAEA Dosimetry Laboratory-Radiation Protection level calibration". The IAEA reference standard chamber LS-01 (#115) used to calibrate the instruments had been calibrated at the BIPM in June 2005 for ^{137}Cs, ^{60}Co gamma.

Radiation quality	Chamber N_K[μGy/nC]	Chamber + electrometer N_K[μGy /scale unit]	$\dot{K}_{air}$ [μGy/min]
^{137}Cs γ-rays*	*25.6 ± 0.2*	*25.6 ± 0.2*	*72*
^{60}Co γ-rays*	*24.6 ± 0.2*	*24.7 ± 0.2*	*8*

*In ^{60}Co and ^{137}Cs γ-rays the chamber is fitted with the build up cap (if applicable).

Uncertainties in the calibration coefficients correspond to a coverage factor, k=2. The calibration coefficients are established at the reference conditions T = 20.0 °C, P = 101.325 kPa and R.H. = 50.0 %.

Settings during the calibration (see Appendix for details):

Electrometer settings at calibration:	*Mode "Charge", Range "High", Pol.sw."minus"*
Scale unit:	*nC*
Polarizing Voltage:	*400 V*
Polarizing Voltage for chamber calibration (alone):	*+400 V (coll.electrode positive)*

Ken R. Shortt

Ken R. Shortt
Head, Dosimetry and Medical
Radiation Physics Section

Date of issue: 2007-09-26

1/2 pages

The reported expanded uncertainty of measurement is stated as the standard uncertainty of measurement multiplied by the coverage factor k=2, which for a normal distribution corresponds to a level of confidence of approximately 95%. The standard uncertainty of measurement has been determined in accordance with ISO guidelines (1995).

This certificate is consistent with the IAEA's capabilities that are recorded in Appendix C of the Mutual Recognition Arrangement (MRA) drawn up by the International Committee for Weights and Measures (CIPM). Under the MRA, all participating institutes recognize the validity of each other's calibration and measurement certificates specified in Appendix C (for details, see http://www.bipm.org).

The Dosimetry Laboratory of the International Atomic Energy Agency is the central laboratory of the IAEA/WHO network of Secondary Standards Dosimetry Laboratories (SSDLs). It provides calibration services to the SSDL members. The Dosimetry Laboratory is operated following a peer-reviewed quality system based on ISO-17025. The IAEA Calibration and Measurement Capabilities have been entered into Appendix C of the MRA.

To sustain its quality system and contribute to the coherence of SI unit for ionizing radiation, the IAEA participates regularly in comparisons organized by regional metrology organizations.

This certificate contains two pages and an Appendix**; it may not be reproduced other than in full. Calibration certificates without signatures and dates are not valid.

International Atomic Energy Agency
Dosimetry and Medical Radiation Physics Section
Division of Human Health, Department of Nuclear Sciences and Applications
Wagramer Strasse 5, PO Box 100
A-1400 Vienna, Austria
Fax: +43 1 26007 21662
Tel.:+43 1 2600 21653

** The appendix can be downloaded from the Internet: http://www-naweb.iaea.org/nahu/dmrp/ssdl.asp

International Atomic Energy Agency

Calibration certificate No. GHA/2007/04

The following instruments from *Ghana Atomic Energy Commission, Radiation Protection Institute Legon, Accra*

have been calibrated at the IAEA Dosimetry Laboratory:

	Ionization chamber	Electrometer
Model/type:	*LS-01*	*UNIDOS*
Serial number:	*227*	*20243*
Manufacturer:	*PTW Freiburg*	*PTW Freiburg*
Calibration period:	from *2007-Apr-05* to *2007-Jun-12*	

Calibration coefficients in terms of air kerma

The calibrations have been performed following the procedure given in Appendix 3B "Ionization Chamber Calibration Procedures at the IAEA Dosimetry Laboratory-Radiation Protection level calibration". The IAEA reference standard chamber LS-01 (#114) used to calibrate the instruments had been calibrated at the PTB in July 2005 for ISO 4037 X ray qualities (narrow-spectrum series).

Radiation quality	Chamber N_K[μGy /nC]	Chamber + electrometer N_K[μGy /scale unit]	$\dot{K}_{air}$ [μGy/min]
X-rays: 40 kV, HVL = 2.7 mm Al	*27.0 ± 0.5*	*26.9 ± 0.5*	*101*
60 kV, HVL = 0.24 mm Cu	*25.4 ± 0.5*	*25.3 ± 0.5*	*177*
80 kV, HVL = 0.59 mm Cu	*25.2 ± 0.5*	*25.1 ± 0.5*	*109*
100 kV, HVL = 1.15 mm Cu	*25.0 ± 0.5*	*24.9 ± 0.5*	*34*
120 kV, HVL = 1.74 mm Cu	*24.9 ± 0.5*	*24.9 ± 0.5*	*45*
150 kV, HVL = 2.40 mm Cu	*24.8 ± 0.5*	*24.8 ± 0.5*	*90*
200 kV, HVL = 4.06 mm Cu	*24.6 ± 0.5*	*24.6 ± 0.5*	*103*
250 kV, HVL = 5.21 mm Cu	*25.0 ± 0.5*	*24.9 ± 0.5*	*129*
300 kV, HVL = 6.19 mm Cu	*25.1 ± 0.5*	*25.0 ± 0.5*	*75*

Uncertainties in the calibration coefficients correspond to a coverage factor, k=2. The calibration coefficients are established at the reference conditions T = 20.0 °C, P = 101.325 kPa and R.H. = 50.0 %.

Settings during the calibration (see Appendix for details):

Electrometer settings at calibration:	*Mode "Charge", Range "High", Pol.sw."minus"*
Scale unit:	*nC*
Polarizing Voltage:	*400 V (polarity switch "minus")*
Polarizing Voltage for chamber calibration (alone):	*+400 V (coll.electrode positive)*

Ken R. Shortt

Ken R. Shortt
Head, Dosimetry and Medical
Radiation Physics Section

Date of issue: 2007-09-26

1/2 pages

The reported expanded uncertainty of measurement is stated as the standard uncertainty of measurement multiplied by the coverage factor k=2, which for a normal distribution corresponds to a level of confidence of approximately 95%. The standard uncertainty of measurement has been determined in accordance with ISO guidelines (1995).

This certificate is consistent with the IAEA's capabilities that are recorded in Appendix C of the Mutual Recognition Arrangement (MRA) drawn up by the International Committee for Weights and Measures (CIPM). Under the MRA, all participating institutes recognize the validity of each other's calibration and measurement certificates specified in Appendix C (for details, see http://www.bipm.org).

The Dosimetry Laboratory of the International Atomic Energy Agency is the central laboratory of the IAEA/WHO network of Secondary Standards Dosimetry Laboratories (SSDLs). It provides calibration services to the SSDL members. The Dosimetry Laboratory is operated following a peer-reviewed quality system based on ISO-17025. The IAEA Calibration and Measurement Capabilities have been entered into Appendix C of the MRA.

To sustain its quality system and contribute to the coherence of SI unit for ionizing radiation, the IAEA participates regularly in comparisons organized by regional metrology organizations.

This certificate contains two pages and an Appendix**; it may not be reproduced other than in full. Calibration certificates without signatures and dates are not valid.

International Atomic Energy Agency
Dosimetry and Medical Radiation Physics Section
Division of Human Health, International Atomic Energy Agency
Wagramer Strasse 5, P.O. Box 100
A-1400 Vienna, Austria
Fax: +43 1 26007-21662
Tel:+43 1 2600 21653

** The appendix can be downloaded from the Internet: http://www-naweb.iaea.org/nahu/dmrp/ssdl.asp